Review article

Photocatalysis as a pre-discharge treatment to improve the effect of textile dyes on human health: A critical review

Dineo A. Bopape [a,*], Bulelwa Ntsendwana [b], Fumani D. Mabasa [c]

[a] Department of Mathematics, Science and Technology Education (DMSTE), University of Limpopo, 0727, South Africa
[b] Nanotechnology Innovation Centre, Advanced Materials Division, Mintek, 200 Malibongwe Drive, Private Bag x 3015, Johannesburg, Gauteng, South Africa
[c] Department of Industrial Psychology and People Management, University of Johannesburg, Soweto, Johannesburg, 1809, South Africa

A B S T R A C T

The increasing need for dyes in the textile sector, has led to significant environmental consequences such as natural water contamination. Textile dyes in water can hinder algae and aquatic plant growth, break down into harmful intermediates, and affect the aquatic food chain. Terrestrial animals may also encounter these dyes through consumption or exposure. Cationic and anionic dyes like methylene blue, malachite green, rhodamine B, methyl orange, eosin y and methyl red can cause skin irritation, carcinogenicity, mutagenicity, and teratogenicity. Therefore, the presence of these dyes in natural and wastewater streams pose significant threats to the aquatic ecosystems, ecological systems and human health. Effective management and remediation of textile dye effluents is crucial to mitigate these risks. Although regulatory bodies like ecological and toxicological association of the dyestuffs manufacturing Industry (ETAD) are working on addressing these risks, more challenges still persist due to nature of textile dyes, lack of enforcement of these regulations on textile dye industries *etc.* and many more. This review explores alternative processes for textile dye effluents treatment before their release to the environment. The aim of the review is to recommend photocatalysis as a suitable preliminary treatment technique for textile effluents before their release to the environment. Photocatalysis stands out amongst other advanced oxidation processes (AOPs) processes as it is a promising approach that researchers worldwide are embracing. It is a process that converts organic pollutants into less harmful substances using light and a photo-excitable catalyst. Both TiO₂ and ZnO are widely used photocatalysts and have shown effectiveness towards dye degradation. Their degradation efficiencies depend on pH, concentration of dye, dosage, time and the type of light. These photocatalysts are reusable and have OH radicals as the most active species during the photodegradation process. Recent studies have shown that photocatalysis, either alone or in combination with other methods like UV or H₂O₂, offers a practical preliminary treatment option for various industrial effluents, enhancing the degradability of complex dyes and pollutants.

1. Introduction

To date, the contamination of water is a persisting problem globally, highlighting the need for continuous evaluation of water

resource policies to tackle this issue [1]. The consequences of water pollution are visible across the world, resulting in deaths and illnesses, with approximately 14,000 individuals losing their lives each day due to water pollution-related causes [1–3]. Both developed and developing nations are facing the complexities posed by water pollution [4,5]. A variety of elements, such as rainfall, weather patterns, soil composition, plant life, geological factors, water flow, groundwater, and human actions, all affect the water quality [5,6]. Research reports that different types of pollutants, including biological, inorganic, and organic contaminants [7–9], can pollute the natural water streams. Despite the various contaminants found in water streams, the organic ones are particularly persistent because they cannot be broken down by natural processes [10]. Inadequate discharge methods lead to the contamination of environmental water by organic pollutants like dyes, making them a major cause of concern [11,12].

The earliest documented dyes were uncovered approximately 1983 BCE [13]. This discovery paved the way for excessive use of indigo dyes in various industries on a large scale [14]. Dyes are commonly employed to add colour to finished products in diverse sectors such as textiles, paper, plastics, *etc.* [15,16]. The demand for inexpensive textiles and clothing since the early 1900s has continuously driven the increasing potential of dyes and colourants as their annual usage surpasses 10,000 tons [14,16,17]. The textile industry is a major player in the global economy, representing more than 6 % of all worldwide exports and providing employment for more than 30 million people globally [18]. Even in extremely small amounts of (1 ppm), these dyes are easily noticeable and unwanted in water [19]. These pollutants can enter the human system via direct and indirect ingestion and they are known to be hazardous to both animals and humans [20–22]. Textile dyes have a significant impact on both human and animal health, with numerous studies documenting their toxic effects [14,15&16]]. These dyes, often resistant to current treatments, pose significant risks to ecosystems and human health through direct exposure and contamination of water supplies [14–17]. Several studies have reported on the impact of textile dyes on the health of both humans and animals and Islam et al. [23] emphasised on the carcinogenicity, mutagenicity, and teratogenicity of these textile dyes, along with their by-products. While a study performed by Islam et al. [24] on Swiss albino mice demonstrated that exposure to wastewater from textile dyeing led to lower haematocrit levels, decreased haemoglobin, and serious reproductive issues such as reduced sperm concentration and structural changes in the testes. Another study found that untreated textile dyes caused severe damage to the liver and intestines of mice, indicating widespread toxicity [25].

Finally, a study by Dutta et al. [26], highlighted that textile dyes can enter the human body through contaminated water or food, resulting in oxidative stress and potential carcinogenicity due to DNA damage. The persistence of these dyes in the environment also leads to a decline in aquatic life, which can indirectly harm human health through the food chain [24]. While these studies highlight the harmful effects of textile dyes, it is important to note that untreated textile wastewater is particularly difficult to manage because of its varied, toxic, and poorly biodegradable components [23]. Methods such as adsorption, coagulation/flocculation, membrane filtration, photocatalysis *etc.* have been utilised to remediate dyes in wastewater. Except for photocatalysis, these methods are expensive, produce secondary contaminants and are subject to fouling [27–29]. Photocatalysis on the other hand, has multiple
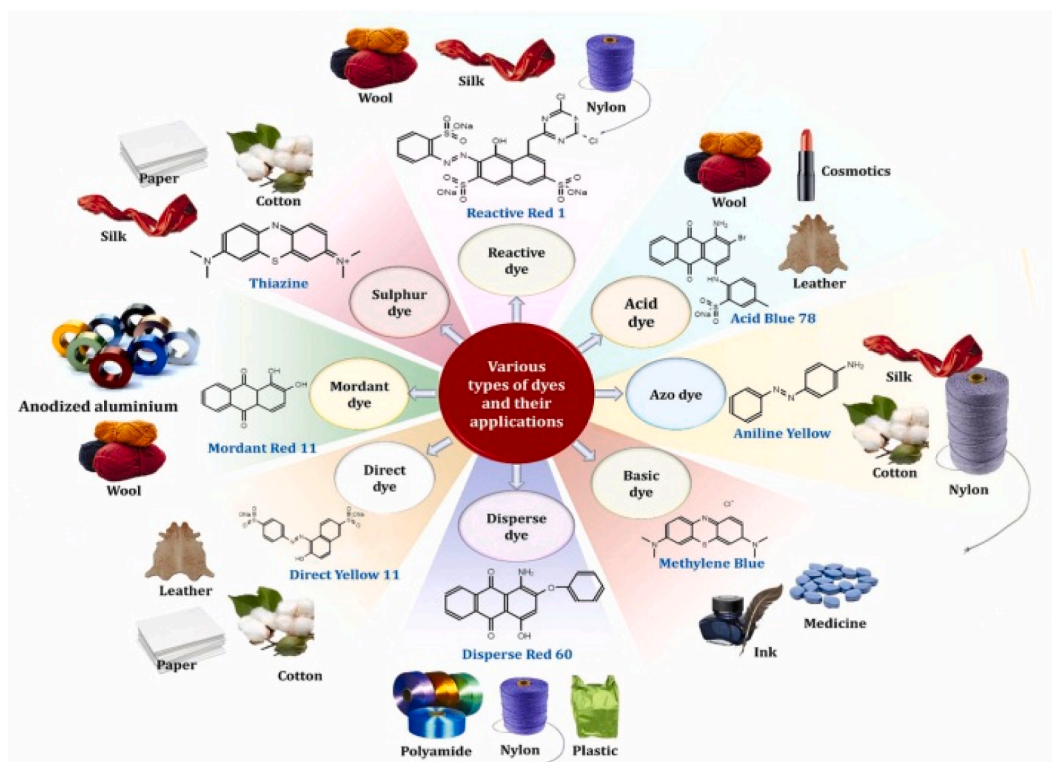

Fig. 1. Types of dyes and their uses. Adapted from Al-Tohamy et al. [39] with license number 5840500084504.

environmental benefits, including complete dye degradation, non-toxic end-products, cost-effectiveness, simplicity, and adaptability in treating a variety of contaminants including heavy metals and organic chemicals [30–33]. The method produces non-toxic end products like CO_2 and H_2O, preventing succeeding contamination [32]. Therefore, photocatalysis has several benefits over conventional treatment methods, making it a potential option for textile dye effluents remediation. The current literature reports on photocatalysis as a new improved method to replace or complement the conventional wastewater treatment methods for textile dye effluents, however, not taking into account the effect of textile dye effluents on the ecosystem of the natural water streams prior treatment. Therefore, this review seeks to report on the impact of textile dye effluents on both human and animal health and recommend photocatalysis as an effective pre-discharge treatment method for textile dye industries. The main emphasis is on both TiO_2 and ZnO as literature reports on their combination with either UV or H_2O_2 as the best pre-discharge remedies for other industrial wastewater effluents.

2. Textile dyes

The high demand for establishing industries that utilise dyes, particularly in the textile sector, has resulted in significant environmental issues. These problems involve the contamination of water and soil; therefore, threatening the lives of both atmospheric and aquatic animals [16,34]. While the textile industry plays a vital role, it consumes large amounts of water and employs over 8000 chemicals at various stages of production, such as washing, bleaching, and dyeing. Consequently, this manufacturing process generates sludge from the textile industry [18,34,and35]]. Studies indicate that the textile industries use approximately a 0.25 billion litres of water daily to produce 8×10^3 kg of cloth [34]. Furthermore, this production converts more than 15 % of the dyes to effluents [14]. These various types of textile effluents are then discharged into the atmosphere and water streams daily.

2.1. Source and classifications of dye effluents

Textile sludge effluents include excessive amounts of organic matter and micronutrients, and they form approximately 80 percent of the entire waste produced by the textile industry [36,37]. World Bank reports the textile industries contribute to contribute above 15 % of overall water pollution during dyeing and finishing processes [38]. Dye substances can be categorized based on their application, chemical properties, origin, physical properties, as well as their application. The classification into the native and synthetic dyes is obsolete at the present time, as it is possible to synthesize various natural dyes. Classifying dyes effluents (Fig. 1) solely based on their application in textiles, leather, paper, and food provides limited information about their properties [39].

A more appropriate way to categorize dyes for different applications is by considering current dyeing technologies such as inks, disperse dyes, pigments, *etc.* [40]. In comparison to other industries, the textile industry discharges 54 % of dyes into the atmosphere, while dyeing contribute 21 %, paper and pulp industry accounts for only 10 %, tannery and paint 8 % and dye manufactures 7 % as depicted in Fig. 2 [14,40].

Textile dye effluents consist of organic materials and contribute significantly to chemical oxygen demand (COD) and biochemical oxygen demand (BOD), requiring considerable attention [18]. Their presence in water inhibits light penetration, resulting to lower dissolved oxygen levels, severely impacting aquatic life as a whole [14,42]. Dyes contain chromophore groups in their molecular structures, which allow them to provide coloration to various materials [43]. They employ polar auxotrophic groups to bind to textile fibres, enabling them to adhere to materials and impart colour [16].

The ecological and toxicological association of the dyestuffs manufacturing Industry (ETAD) worked in partnership with governments to tackle the concerns related to the toxic effects of textile effluents [12]. Approximately 90 % of the 4000 dyes evaluated in an ETAD research had a median fatal dose value greater than 2 g/kg, with basic and direct dyes showing the greatest levels of toxicity. Dyes cannot be easily remediated in water due to their aromatic structure and non-biodegradability, thereby posing substantial environmental and health risks [41]. Therefore, it is important to remediate these harmful substances before they could reach the environment to address concerns related to environmental safety and toxicity [14].
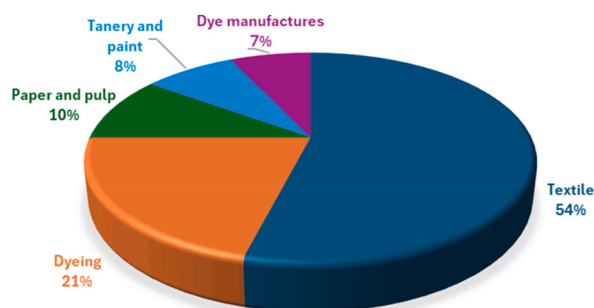

Fig. 2. Industries responsible for releasing dye wastewater into the environment and their percentage contribution [41].

2.2. Textile dyes

Textile dyes released into water decrease light penetration, which can hinder the growth of algae and aquatic plants [39]. Additionally, when fish and other organisms consume these dyes, they can be broken down into harmful intermediates within their bodies, therefore, affecting the physical condition of the entire aquatic food chain [38,41]. Terrestrial animals may potentially come into touch with azo dyes by consuming or through direct exposure to industrial effluent [42,44]. Fig. 3 shows the ecotoxicological effects of textile dye effluents [39].

Dyes utilised in the textile industry are divided into different classes and groups according to their overall dye structure, origin, and compatibility with different types of fibres [44]. The largest group of colorants, known as azo dyes, makes up ~60 % of all industrial dyes employed. Regarding their structural representations, dyes are further divided (as shown in Fig. 4) into cationic or anionic types [45]. Various studies discussed the toxicological effect of these textile dyes on humans and animals (Table 1) [41].

Table 1 reports on the potential risks imposed by textile dyes on both humans and animals' health. Textile dyes are categorized into basic (cationic), anionic (acidic), reactive and sulphur types based on their chemical structure. Their toxicity ranges from skin and eye irritation to carcinogenicity, mutagenicity, and teratogenicity. Examples include Methylene Blue and Rhodamine B, which cause skin irritation, and Rose Bengal and Congo Red, known for their mutagenic and carcinogenic characteristics. Reactive Red 120 and reactive Blue 15 known for their genotoxic, mutagenic and carcinogenic nature ad lastly sulphur black and amido black are known to disrupt the aquatic ecosystem and their carcinogenic nature. This review focuses more deeply into cationic and anionic dyes. The release of these cationic and anionic textile dyes into aquatic environments poses significant threats to ecological systems and human health. Effective management and remediation of these dye effluents are crucial to mitigate these risks.

Cationic dyes, including MB, MG, and RhB which are popularly utilised in dyeing fabrics can ionise into positively charged ions in aqueous solutions [12]. In contrast, anionic textile dyes like MO, CR, and EY are also widely used in textile factories and dissociate into negatively charged ions in aqueous solutions [80].

The nature, toxicological impact and environmental impact of the cationic and anionic dyes are explained further in the following sections.

2.2.1. Cationic textile dyes

The first cationic dye to be discussed is malachite green (MG, Fig. 4), it is a synthetic triphenylmethane dye of a deep green colour.
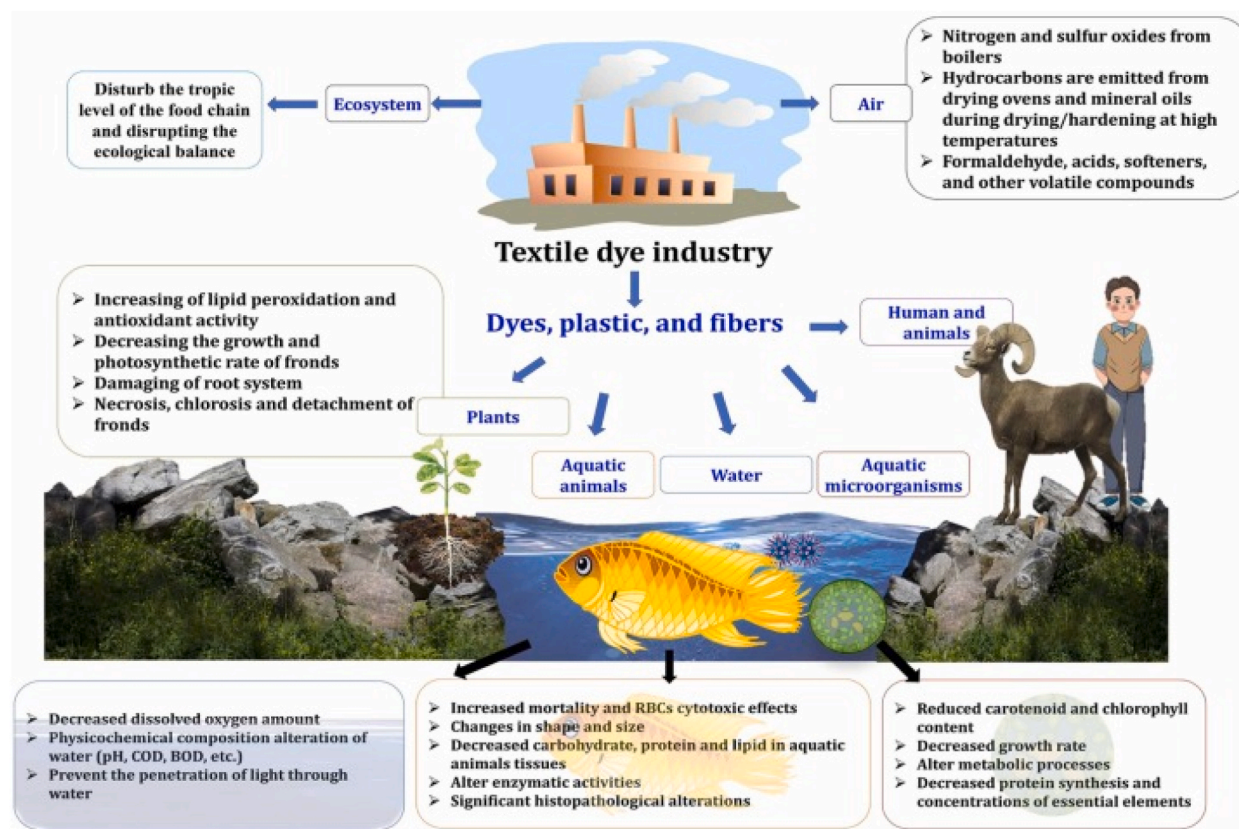

Fig. 3. Ecotoxicological effects of textile effluent on the about the atmosphere and organisms. Adapted from Al-Tohamy et al. [39] with license number 5840500084504.
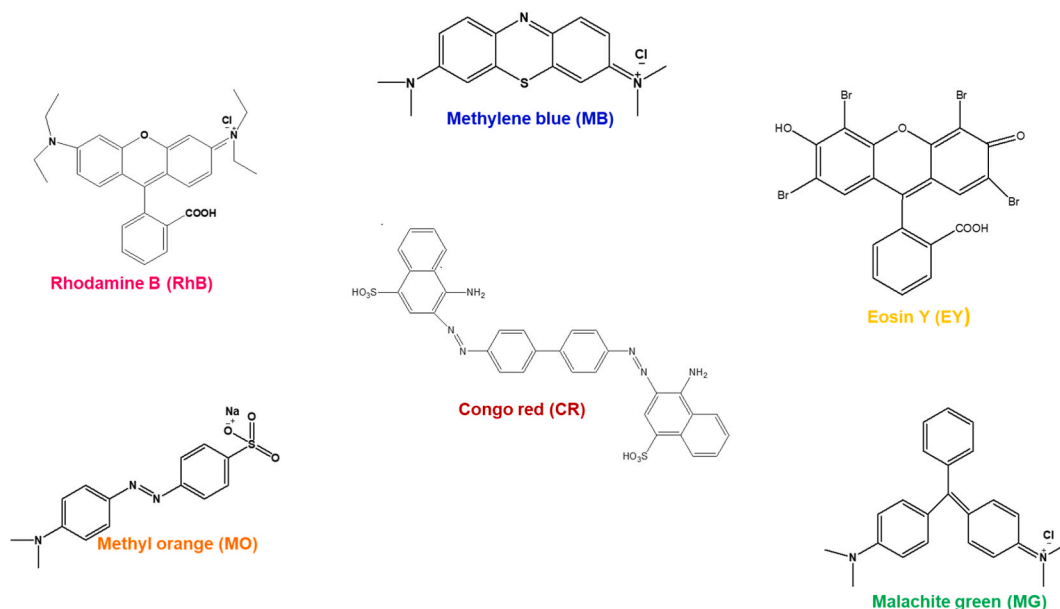
Fig. 4. Examples of textile dyes [45].

It can be dissolved in water and is utilised across various industries [81–85]. Its primary applications include dyeing textiles, cosmetics, papers, foods, and pharmaceuticals [81–84,86]. In fish farming, MG is employed as an agent to combat fungal and protozoan diseases, serving as an anti-parasitic, anti-fungal, and anti-bacterial substance [82–84,87]. Nevertheless, excessive levels of MG have been found to have harmful effects on various organs of aquatic organisms [61]. While certain countries have prohibited the usage of this dye, others have excessively used it due to its affordability and effectiveness [81,86]. This dye is highly aromatic, stable, and non-biodegradable in nature, hence there has been significant interest in remediating it from water resources [87–89].

The second cationic dye is rhodamine B (RhB, Fig. 4), RhB finds extensive applications and it is extensively used in field of biology, chemistry, and optics [90]. It was initially used as a colouring agent in fabrics and foods but is now widely employed as a fluorescent tracer in water [91]. RhB is highly valued for its exceptional stability as a dye laser material and its effectiveness as a biological stain [92]. Additionally, industries like paper printing and leather also utilise RhB [93]. This bright bluish-red dye is classified as a basic cationic dye that can be dissolved in water and ethanol [92,94]. However, Rhodamine B can be harmful to both humans and animals if ingested, causing irritation to the sensory system and respiratory tract [91–93]. The Environmental Protection Agency (EPA) has designated RhB as a list I inert substance, classifying it as a compound that is carcinogenic, reproductive toxic, neurotoxic, and developmentally toxic [95]. As a result of its potential hazards and carcinogenic properties, the use of this dye has been prohibited in the food and cosmetics industry [92]. Consequently, there is an urgent need to effectively eliminate Rhodamine B from water sources.

The final dye to discuss is methylene blue (MB, Fig. 4), MB is commonly used for staining biological samples and colouring materials like paper, hair, cotton, and wool [96]. MB was synthesized by Caro et al. in 1876 as an artificial dye for colouring cotton, making it one of the earliest synthetic dyes developed [97,98]. This compound, with the chemical formula $C_{16}H_{18}N_3SCl$, has heterocyclic properties and is effective in staining and deactivating microbial species [99]. It is observed as a dark green solid but turns blue when dissolved in water [99]. MB injections are utilised for treating methemoglobinemia and urinary tract infections [100]. Additionally, in 1932, it was discovered as a remedy for carbon monoxide and cyanide poisoning [99].

Methylene blue is categorized as a toxic pigment, and it is reported to be harmful to both human and animal health [101]. The direct ingestion or contact of MB in can cause eye and skin irritation, vomiting, diarrhoea, *etc.* [97]. Ingestion of MB in humans may result in symptoms like jaundice and quadriplegia [102,103]. In a mouse experiment, the level of MB that did not cause any observed adverse effects (NOAEL) was found to be 25 mg/kg [104]. The aromatic nature of MB makes it resistant to biodegradation through conventional water treatment methods. The Environmental Protection and Management (Trade Effluent) Regulations stipulate that dye effluent cannot be disposed into streams or onto the environment without prior written consent from the Director-General [105]. Therefore, permissible levels of MB vary based on the regulatory agency and local jurisdiction. The Environmental Protection Agency (EPA) provides general guidelines, suggesting a limit of 0.2 mg/L [105]. However, in many countries, such as South Africa, there are no specific regulations governing the permissible levels of MB in wastewater resources. Therefore, it is crucial to eliminate or remediate MB from effluents before their discharge into freshwater systems becomes necessary.

2.2.2. Anionic textile dyes

As an anionic dye, Congo red (CR, Fig. 4), has previously been linked to allergic reactions [106]. CR strong attraction to cellulose fibres makes it valuable in the textile industry [107]. Reports show that CR is widely employed across multiple industries, such, printing, rubber, cosmetics, leather, pulp, textile, plastics, paper, and biomedical laboratories. Consequently, significant amounts of CR

Table 1

Toxicological data on several textile dyes.

Dye name	IUPAC name	Chemical formula	Type	Toxicity	Refs
Methylene Blue (MB)	[7-(dimethylamino) phenothiazin-3-ylidene]-dimethylazanium; chloride	$C_{16}H_{18}ClN_3S$	Basic	Eye and skin irritant	[45,46]
Rhodamine B (RhB)	N[9-(ortho-carboxyphenyl)-6-diethylamino-3H-xanthen-3-ylidene]	$C_{28}H_{31}ClN_2O_3$	Basic	Causes skin irritation	[47,48]
Rose Bengal (RB)	4,5,6,7-tetrachloro-2′,4′,5′,7′-tetraiodo fluorescein	$C_{20}H_4Cl_4I_4O_5$	Acidic	Carcinogenic	[49,50]
Congo Red (CR)	Disodium-4-amino-3-[4-(4-(1-amino-4-sulfonato-naphthalen-2-yl)diazenylphenyl)-phenyl]-diazenyl-naphthalene-1-sulfonate	$C_{32}H_{22}N_6Na_2O_6S_2$	Acidic	Carcinogenic and mutagenic	[51,52]
Methyl Orange (MO)	Sodium-4-{[4-(dimethylamino)-phenyl] diazenyl}-benzene-1-sulfonate	$C_{14}H_{14}N_3NaO_3S$	Acidic	Carcinogenic, genotoxic, mutagenic	[53,54]
Acid Violet 7 (AO7)	5-acetamido-3-[-(4-acetamidophenyl)-diazenyl]-4-hydroxynaphthalene-2,7-disulfonic acid	$C_{20}H_{16}N_4$ $Na_2O_9S_2$	Basic	Causes degradation of lipid, chromosomal abnormality	[55–57]
Methyl Red (MR)	2-{[4-(Dimethylamino)phenyl]diazenyl} benzoic acid	$C_{15}H_{15}N_3O_2$	Acidic	It irritates the skin, eyes, respiratory system, and digestive tract.	[58–60]
Remazol Brilliant Blue R (RBBR)	Disodium-1-amino-9,10-dioxo-4-{3-[2-(sulfonatooxy)-ethane-1-sulfonyl]-anilino}-9,10-dihydroanthracene-2-sulfonate	C22H16 N2Na2O 1S3	Basic	Carcinogenicity, genotoxicity, mutagenicity	[61,62]
Eosin Y (EY)	Disodium-2-(-2,4,5,7-tetrabromo-3-oxido-6-oxoxanthen-9-yl) benzoate	$C_{20}H_6Br_4Na_2O_5$	Acidic	Carcinogenic, causes swelling and redness of eyes	[63, 64&65]
Malachite Green (MG)	4-{-[4-(Dimethylamino)-phenyl]-(phenyl)-methylene}-N,N-dimethyl-2,5-cyclohexadien-1-iminium chloride	$C_{23}H_{25}ClN_2$	Basic	cytotoxic, carcinogenic and teratogenic	[66,67]
Crystal Violet (CV)	4-{Bis-[4-(dimethylamino)-phenyl]-methylidene}-N,N-dimethylcyclohexa-2,5-dien-1-iminium chloride	$C_{25}H_{30}ClN_3$	Basic	Carcinogenic and mutagenic	[68–70]
Reactive Red 120 (RR120)	5-[[4-chloro-6-[4-[[4-chloro-6-[[8-hydroxy-3,6-disulfo-7-[(2-sulfophenyl)diazenyl]naphthalen-1-yl]amino]-1,3,5-triazin-2-yl]amino]anilino]-1,3,5-triazin-2-yl]amino]-4-hydroxy-3-[(2-sulfophenyl)diazenyl]naphthalene-2,7-disulfonic acid	$C_{44}H_{24}Cl_2N_{14}O_{20}S_6Na_6$	Reactive	Genotoxic, damages root cells (plants) and DNA cells (fish).	[71,72]
Reactive Black 5	tetrasodium; 4-amino-5-hydroxy-3,6-bis[[4-(2-sulfonatooxyethylsulfonyl)phenyl]diazenyl]naphthalene-2,7-disulfonate	$C_{26}H_{21}N_5Na_4O_{19}S_6$	Reactive/ Sulphur	affects respiratory system, bronchitis, irritate skin and bladder cancer	[71,73]
Reactive Orange 16 (RO16)	disodium; 6-acetamido-4-hydroxy-3-[[4-(2-sulfonatooxyethylsulfonyl)phenyl]diazenyl]naphthalene-2-sulfonate	$C_{20}H_{17}N_3Na_2O_{11}S_3$	Reactive/ Sulphur	Rash, cancer, fever and dermatitis.	[71,74]
Reactive Blue 15 (RB15)	tetrasodium [[[[5-[(4-amino-6-chloro-1,3,5-triazin-2-yl)amino]-2-sulphophenyl]amino]sulphonyl]-29H,31H-phthalocyaninetrisulphonato(6-)-N29,N30,N31,N32]cuprate(4-)	$C_{41}H_{23}ClCuN_{14}O_{14}$	Reactive	Carcinogenic and mutagenic	[71,75]
Reactive Red 198 (198)	tetrasodium; 5-[[4-chloro-6-(3-sulfonatoanilino)-1,3,5-triazin-2-yl] amino]-4-hydroxy-3-[[4-(2-sulfonatooxyethylsulfonyl)phenyl]diazenyl]naphthalene-2,7-disulfonate	$C_{27}H_{18}ClN_7Na_4O_{16}S_5$	Reactive/ Sulphur	Allergenic, carcinogenic and mutagenic.	[71,76]
Sulphur Black 1	2,10-dinitro-12H- [1,4]benzothiazino [3,2-b] phenothiazin-3-one	$C_{18}H_8N_4O_5S_2$	Sulphur	inhibitory effects on plant growth and affects soil microbiota	[77,78]
Amido black	sodium; 4-amino-5-hydroxy-3-[(4-nitrophenyl)diazenyl]-6-phenyldiazenylnaphthalene-2,7-disulfonic acid	$C_{22}H_{16}N_6NaO_9S_2$	Sulphur	Carcinogenic	[77,79]

are released into water sources without undergoing proper treatment [108,109]. Despite its benefits, CR is highly poisonous and carcinogenic when present as a negatively charged dye [110]. Inadequate disposal of CR leads to environmental contamination, presenting challenges for environmental protection agencies (EPA). Therefore, it is crucial to develop an effective approach for breaking down CR in water resources.

While methyl orange (**MO, Fig. 4**) has been widely used as a dye pigment because it is an acidic anionic dye, sometimes referred to as an azo dye [111,112]. It is also textile, paper, food, and leather, and as an indicator in scientific research [111–115]. Its IUPAC name is 4-dimethylaminoazobenzene-4-sulphate [111]. The discharge of wastewater from these industries, even when containing small amounts of the dye, are hazardous to the lives of organisms [113]. MO not only jeopardizes human health but also disrupts the ecological balance, primarily due to its highly mutagenic toxicity, which can lead to cancer and genetic damage [111,115]. In case of accidental ingestion, specific enzymes called reductases present in the intestines and liver can trigger the breakdown of the azo group within MO [114]. This breakdown forms amines belonging to aromatic compounds, which are carcinogenic and particularly contribute

to the development of intestinal cancer [112,114]. Extensive evidence suggests that MO poses substantial risks, including harm to the eyes, which can result in long-lasting damage [115]. The presence of methyl orange in wastewater hampers effective biochemical purification, making its degradation a challenging task [111]. Thus, it is crucial to employ advanced processes to degrade this harmful dye used in the textile industry.

Eosin Y (EY, Fig. 4) is a commonly used azo dye that carries a negative charge and contains bromine atoms [116]. EY is highly soluble in water and can readily enter red blood cells [117]. It finds extensive applications as an organic dye in environmental and pharmaceutical research, often employed to assess the effectiveness of different adsorbents for comparison purposes [118,119]. In the process of gram staining, Eosin Y is commonly used to distinguish between different bacterial species and as a colouring agent [117, 118]. Additionally, it is frequently used in the textile sector as a pigment in formulas for fluorescent dyes and printing [116]. Moreover, EY serves as a photocatalyst, neutralizer of biological substances, stabilizer in mini-emulsion systems, and spectroscopic probe for examining specific properties or phenomena [118]. However, a significant amount of EY dye is lost during assembly and preparation processes, eventually finding its way into water resources through wastewater [116]. The toxicological properties of EY indicate it's a skin and eyes irritant, resulting in redness and discomfort. Furthermore, it damages the eyes, kidneys and liver [117]. Consequently, the release of a substantial quantity of Eosin Y into the environment poses potential challenges to water quality and ecosystem health [116,119]. Posing a need to develop a suitable method to remediate RY in water sources.
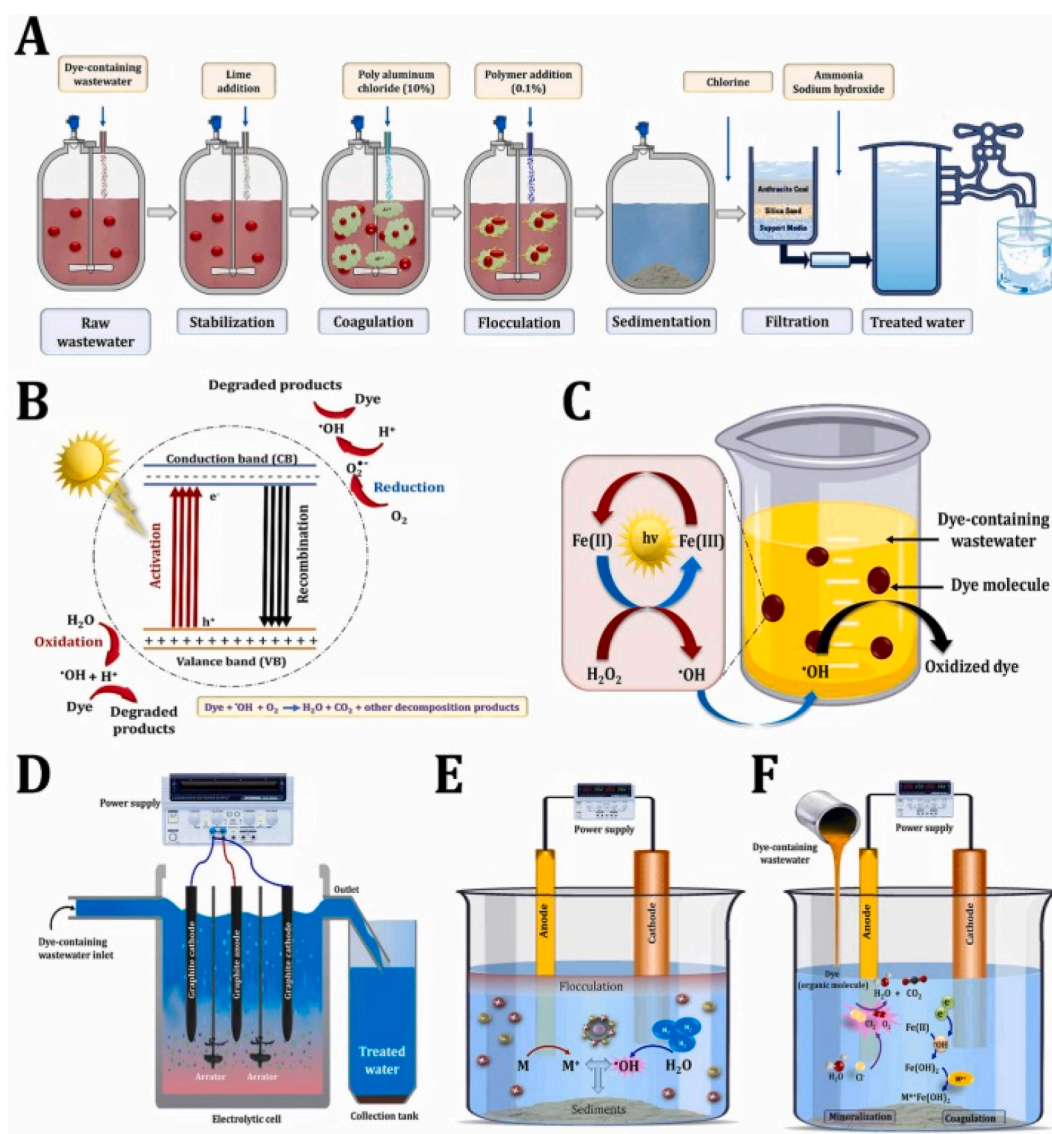

Fig. 5. Chemical methods for treating dye effluents include coagulation-flocculation (a), photocatalysis (b), photo-Fenton (c), electro-Fenton (d), electrocoagulation (e), and oxidation (f). Adapted from Al-Tohamy et al. [39] with license number 5840500084504.
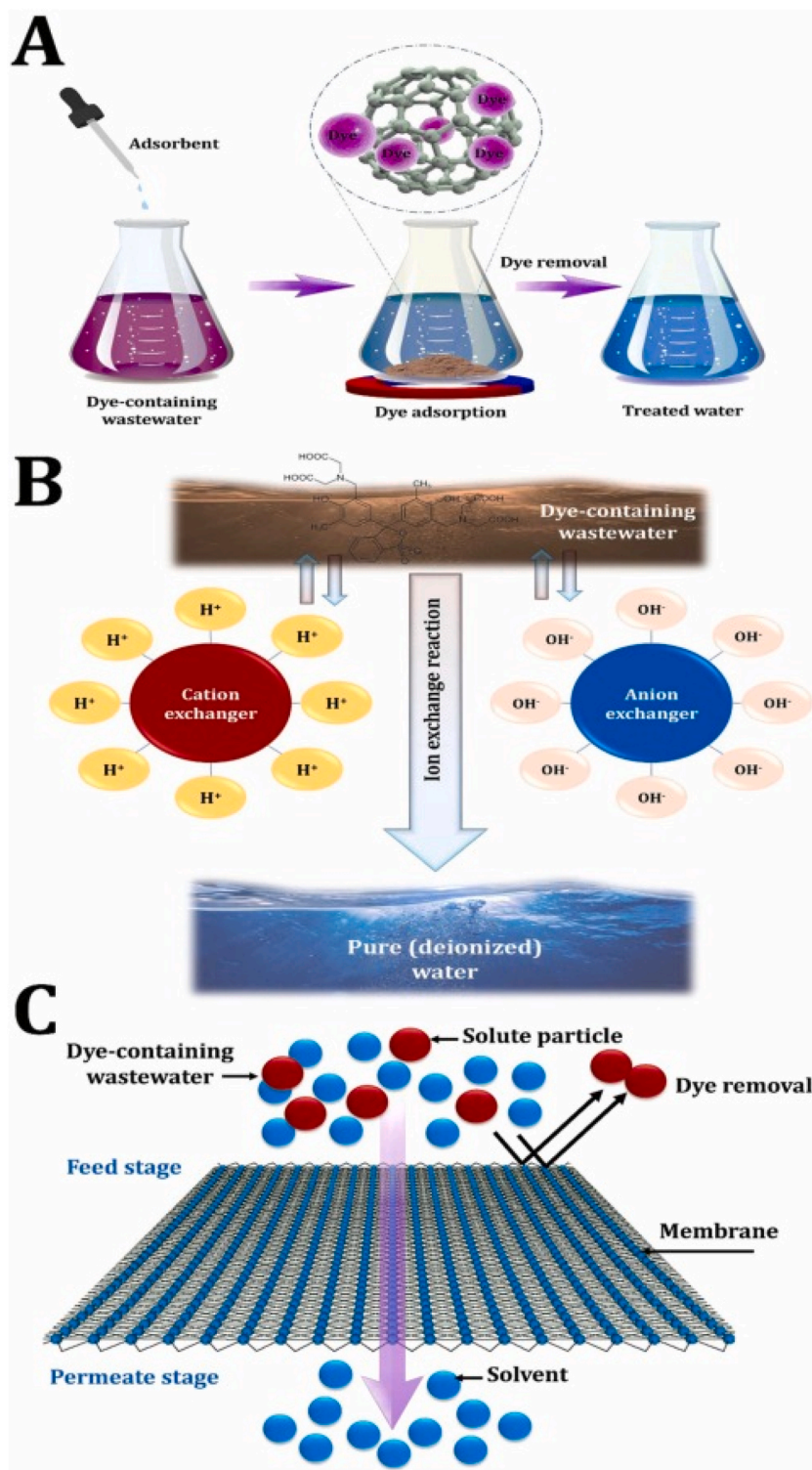
Fig. 6. Textile dye effluent treatment methods (a) adsorption, (b) ion exchange, and (c) membrane filtration. Adapted from Al-Tohamy et al. [39] with license number 5840500084504.

3. Conventional treatment methods

Numerous countries worldwide still lack adequate discharge regulations and guidelines for most textile dyes [120–123]. To address this issue, various conventional treatment methods (Fig. 5a) were used to degrade these contaminants from water [39]. These conventional treatment methods include coagulation/flocculation, membrane filtration, and ion exchange [124–127].

3.1. Coagulation/flocculation (CF) process

In coagulation/flocculation (CF), larger molecules aid in the accumulation and settling of flocs, resulting in the formation of bigger flocs during the coagulation procedure (Fig. 5a). Subsequently, the flocs solidify and settle at the bottom during the flocculation process [128]. While CF is widely used by water treatment plants, studies indicate that this technique is more effective in removing suspended and dissolved particles, colloids, and organic materials, which are commonly found in industrial effluents [129]. However, CF has inherent disadvantages, such as equipment staining caused iron and aluminium salts. Moreover, the chemical coagulants commonly used in CF can be harmful to the environment and increase operational expenses.

3.2. Membrane filtration (MF) technique

The membrane separation/membrane filtration process (MF) is performed at room temperature (Fig. 6c) and does not generate by-products; therefore, it is regarded as a cost-effective and highly efficient separation method [130]. MF is commonly used to remove auxiliary chemicals, salts, and colours [131]. However, there are still limitations and areas that require improvement, such as enhancing membrane performance in terms of permeability, selectivity, antifouling properties, and scaling prevention [130,131]. The usefulness of reverse osmosis (RO) membranes is hindered by significant variations in osmotic pressure.

3.3. Ion exchange technique

Ion exchange (Fig. 6b) involves the exchange of negative and positive ions placed on a solid sorbent in a solution [132]. This process prefers using resins which are commercially available to treat the dye wastewater [133]. However, the ion exchange processes are conducted in costly fixed beds and suffer from low flux. Another drawback of ion exchange resins is the need for disposal or regeneration of the sorbent material [134].

3.4. Adsorption techniques

Adsorption (Fig. 6a) involves the accumulation of various particles from wastewater pollutants onto the surface of an adsorbent [135,136]. This technique is attractive for removing dyes because it is cheap and flexible in design [135]. Many textile industries utilise commercial activated carbon, clays etc. as adsorbents for treating dye waste [136]. However, most of these adsorbents are environmentally unfriendly, ineffective against various dyes, and can generate secondary contaminants known as sludge [137,138].

Removal of dyes in water using conventional methods was carried by various studies (Table 2).

Ihaddaden et al. [139] concentrated on the impact of many parameters on the coagulation/flocculation dye treatment process, including the masses of biomaterials, pH, settling duration, MB concentration *etc*. The highest dye removal of 98.29 % was achieved in 19 min. It is interesting to observe that pH had no discernible effect on the MB removal.

While Moghaddam et al. [140], utilised the ferric chloride sludge (FCS) in removing acid red 119 (AR119) dye from wastewater.

Table 2
Removal of dyes using various conventional treatment methods.

Technique	Dye	Time	% Removed	References
Coagulation/Flocculation	MB	19 min	98.29	[139]
	AR119	67 min	96.53	[140]
	AB92	128 min	99	[141]
Membrane filtration	MG	–	88.21	[142]
	MB	–	83.91	
	CV	–	71.99	
	MB	–	99.61	[143]
	EBT	–	90.86	
	MB	–	98	[144]
Ion exchange	MB	5 min	94.6	[145]
	EB	1440 min	99.56	[146]
Adsorption	MO	30 min	68.6	[147]
	MB	4 h	97	[148]
	RhB	24 h	>90	[149]
	CR	24 h	>90	
	MB	120 min	94	[150]
	CV	120 min	94	

They also researched parameters such as pH, dosage of the FCS, and the concentration of the AR119 dye. The optimized conditions led maximum dye removal of 96.53 % after 67 min.

The research done by Szyguła et al. [141], utilised chitosan to treat coloured solutions through a process called coagulation-flocculation. A sulfonic dye known as Acid Blue 92 was used as a model to evaluate the dye's capacity to remediate textile effluent. The result revealed that chitosan demonstrated higher colour removal efficiency in tap water compared to demineralized water. Interestingly, tap water required a significantly lower chitosan concentration to achieve the desired results. Under the optimal conditions, the maximum dye removal reached 99 %.

Wu et al. [142], utilised chitosan (CS), polyvinylpyrrolidone (PVP), and polyvinyl alcohol (PVA) to successfully synthesize a hollow nanofiber membrane (CS/PVP/PVA-HNM) using a coaxial electrospinning method. The rejection ratios of CS/PVP/PVA-HNM for several compounds, including methylene blue (MB), malachite green (MG) and crystal violet (CV), were determined to be 83.91 %, 88.21 %, and 71.99 %, respectively.

The research done by Subrahmanya et al. [143], presented a syringe filter membrane that is environmentally friendly,
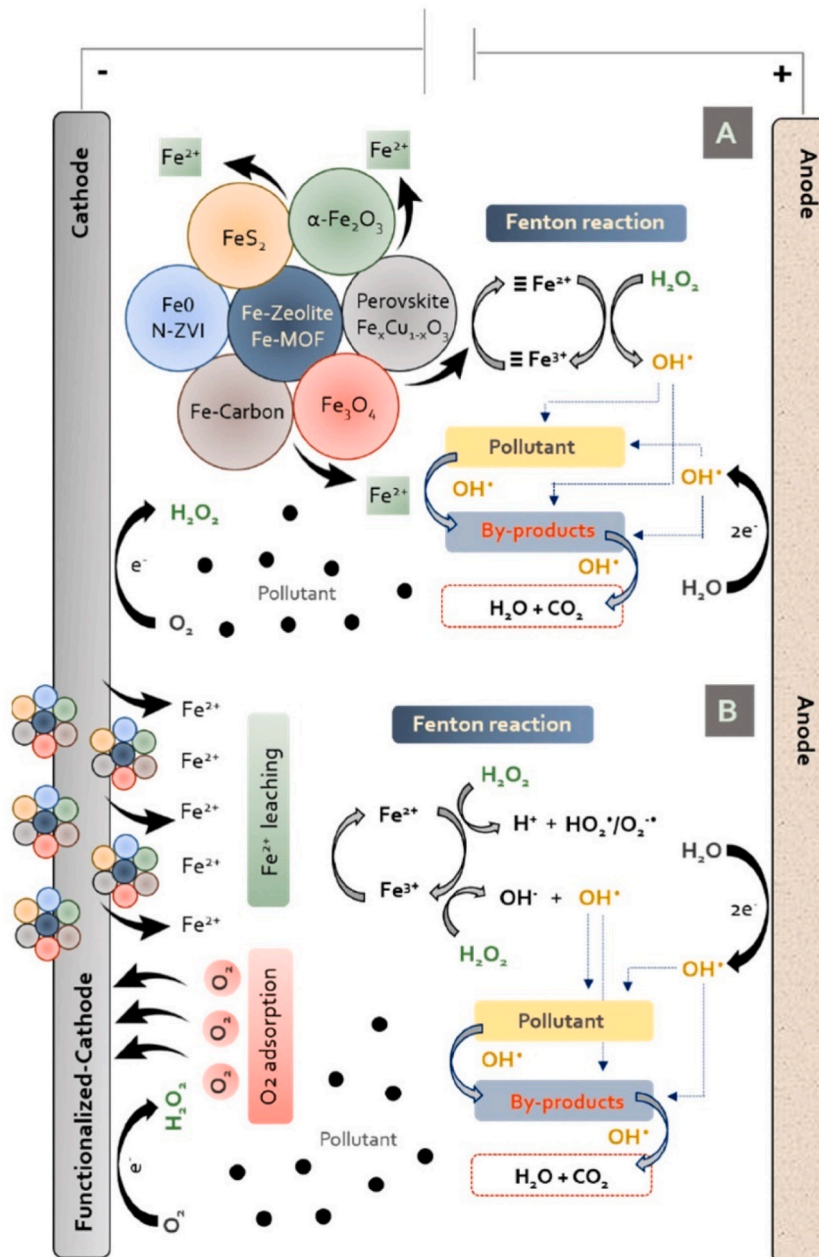

Fig. 7. The mechanism underlying the catalytic activation in the electro-Fenton process. Adapted from Meijide et al. [161] with CC BY licence.

cost-effective, and can be used multiple times. The membrane was composed of a mixture of polydopamine (PDA), graphene oxide (GO) and encapsulated mesoporous silica (SBA-15-PDA). This optimized $GO_{10}/(SBA-15/PDA)_2$ membrane effectively removal 90.86 % (EBT) and 99.61 % (MB) in wastewater.

Zhu et al. [144] have proposed a new method for removing dyes from saline solutions by membrane filtration process. The process involves dissolving a polyacrylonitrile nanofiber membrane with ethanolamine and immersing it in water to solidify the channels. The effectiveness of these channels in dye rejection was evaluated, with methyl blue (MB) removal efficiency of 98 %.

In another research, Joseph et al. [145] studied the efficiency of an ion exchange resin composed of micro-sized ammonium phosphomolybdate (APM) particles. The APM effectively removed 94.6 % MB dye from water within 5 min and it maintained a removal efficiency up to the 16 cycles. The APM resin was pH sensitive but not light sensitive, therefore, the process of dye removal was adsorption and not photocatalysis.

Khan et al. [146], researched the percentage of removal of eosin-B (EB) dye using BIII (QPPO/PVA-based system). A number of parameters were analysed, and the percent of EB removed with 0.1 g of BIII and 1440 min was 99.56 %. Furthermore, the membrane's effectiveness remained constant even after four consecutive cycles of usage, demonstrating that it is reusable.

Zhang et al. [147] synthesized a hollow polyphosphazene microcapsule, rich in amino content and with a rigid-flexible coupling cationic skeleton (HTCM) in a single step through polycondensation using hexachlorocyclotriphosphazene and tetraethylenepent-amine. The HTCM reached a maximum adsorption efficiency of 67 % of methyl orange (MO) within 30 min.

The research by Hu et al. [148], introduced a new type of cotton fabric called superhydrophilic and underwater superoleophobic cotton fabric (SUSCF). Interestingly, the incorporation of CNT, PSS, and PDA into the SUSCF achieved a maximum 97 % removal ratio of MB.

Do et al. [149], focused on preparing graphene-like carbon (GLC) from biomass as an eco-friendly and straightforward approach. The GLC over 90 % removal of CR and RhB dyes.

Rani and Chaudhary [150] explored the *Citrus limetta* peel (ACLP) as an adsorbent for removing MB and CV dyes. They optimized the process showed that with 0.1 g of ACLP, ~83 % of MB and ~90 % of CV dyes were removed in 120 min at a pH of 7. The pseudo-second-order model was followed by this process therefore suggesting a chemisorptive nature.

Overall, these traditional approaches for removing textile dyes, have drawbacks and constraints [149–152]. These include inadequate removal of dyes, creation of harmful substances, substantial energy and chemical demands, sensitivity to pH and temperature, prolonged treatment durations, limited efficacy with specific dyes, production of sludge or waste, and a lack of adaptability [152,153]. Nonetheless, continuous research and technological progress are augmenting the efficiency and efficacy of dye removal processes. Additionally, alternative and advanced treatment methods like, advanced oxidation processes are under investigation to address these limitations.

4. Advanced oxidation process

Advanced oxidation processes (AOPs) (Fig. 5b-f) are highly effective in treating a variety of toxic organic/inorganic pollutants and fully eliminating nonbiodegradable contaminants such dyes, pharmaceuticals, pesticides, *etc.* [154].

These AOPs, are applied in industrial settings, hospitals, and wastewater treatment plants to treat toxic effluents effectively [154, 155]. AOPs encompass several methods, such as Fenton, photo-Fenton, sonolysis, photocatalysis, *etc.* [156]. Glaze et al. [157] first introduced AOPs, emphasizing the role of hydroxyl radicals in purifying water. The definition, evolution, and varied strategies for creating •OH radicals and other reactive oxygen species such O_2^{2-}, H_2O_2, and $1O_2$ during the process were comprehensively examined [158]. However, it is critical to note that •OH radicals are the most efficient and potent species in AOPs.

4.1. Electrochemical

The Fenton system, including the Fenton and Fenton-based approach (Fig. 5c–d), constitutes an advanced variant of the AOP (Advanced Oxidation Process). In this methodology, electromagnetic radiation like UV light is incorporated alongside the conventional Fenton process, which employs the Fe^{2+}/H_2O_2 reagent. This technique is widely recognized for its ability to generate hydroxyl radicals (•OH) in situ under acidic conditions, which exhibit potent oxidation capabilities [159,160]. These hydroxyl radicals, known for their strong oxidative properties, interact non-selectively with various electron-rich organic molecules, leading to the formation of CO_2, H_2O, and several intermediate compounds (Fig. 7) [141].

Despite the Fenton system's merits in removing diverse pollutants, it suffers from several drawbacks. These include a limited pH range of 3–5, the persistence of iron ions causing residual coloration in treated water, challenges in large-scale production of H_2O_2, and elevated treatment costs [139]. Additionally, the system's reaction rate is hindered by sluggish mass transfer rates between the electrode's active surface and the bulk solution [141]. The drawbacks associated with the methods render them less appealing for tackling the removal of dyes and antibiotics.

4.2. Sonochemical

Recent studies have demonstrated the remarkable efficacy of ultraviolet (UV)-based advanced oxidation processes (AOPs) in treating wastewater [162–164]. One particularly attractive method is the UV/H_2O_2 process, which generates the highly reactive and non-selective •OH radical [162–166]. This radical plays a key role in breaking down organic contaminants through direct UV photolysis in the UV/H_2O_2 process [162,166,167]. Despite its success, there are practical challenges that need to be addressed. The (i)

H_2O_2 tends to be unstable in water solutions, leading to the generation of O_2 instead of the desired HO• radical; (ii) H_2O_2 rapidly decomposes under UV light, posing difficulties in control and reducing its efficiency; and (iii) H_2O_2's corrosive and unstable nature hinders its transport and use during treatment processes [168,169]. Among various methods discussed, photocatalysis stands out as a promising approach that researchers worldwide are embracing. This technique has gained popularity for efficiently breaking down dyes and pharmaceuticals in both natural water bodies and wastewater [164]. It is quick, easy to use and does not produce secondary sludge [170].

4.3. Photocatalysis

Photocatalysis is a popular process that uses light alongside a photo-excitable catalyst material to transform organic pollutants into less harmful substances [171]. This process involves a photocatalyst composed of a band gap between the valence band (VB) and a conduction band (CB). This band gap represents the energy required to energize the movement of electrons between the VB and CB levels.

In the typical photocatalytic MB dye degradation process of TiO_2 (Fig. 8), there are various steps involved:

4.3.1. Photon absorption
As seen on **equation (1)**, the first step occurs when sufficient light (UV/Vis) is absorbed by the TiO_2, this light energy (photon) is ether equal to or greater than its bandgap energy of 3.4 eV. The electrons in the valence band (VB) become excited and move to the conduction band (CB), leaving behind positive holes in the VB [170].

$$TiO_2 + hv \rightarrow e_{CB}^- + h_{VB}^+ \tag{1}$$

4.3.2. Formation of electron-hole pairs
The resulting electrons (e^-) and holes (h^+) produced form the electron-hole pairs which are highly reactive and are important for various reactions [171].

4.3.3. Migration charge carrier
The photogenerated electrons (e^-) and holes (h^+) travel to the surface of the TiO_2, where they interact with molecules like oxygen (O_2) and water (H_2O). For an efficient photodegradation process it is crucial for the electron-hole pairs do not recombine before reaching the surface of the photocatalyst, as they need to form reactive species [173].

4.3.4. Formation of reactive oxygen species (ROS)
The e^- and h^+ initiate redox reactions on the surface of TiO_2, generating highly reactive oxygen species (ROS) such as superoxide radicals (•O_2^{2-}) as shown in **equation (2)** and hydroxyl radicals (•OH) as shown in **equation (3)**, which are responsible for MB dye degradation occurring in two separate redox reaction [172].
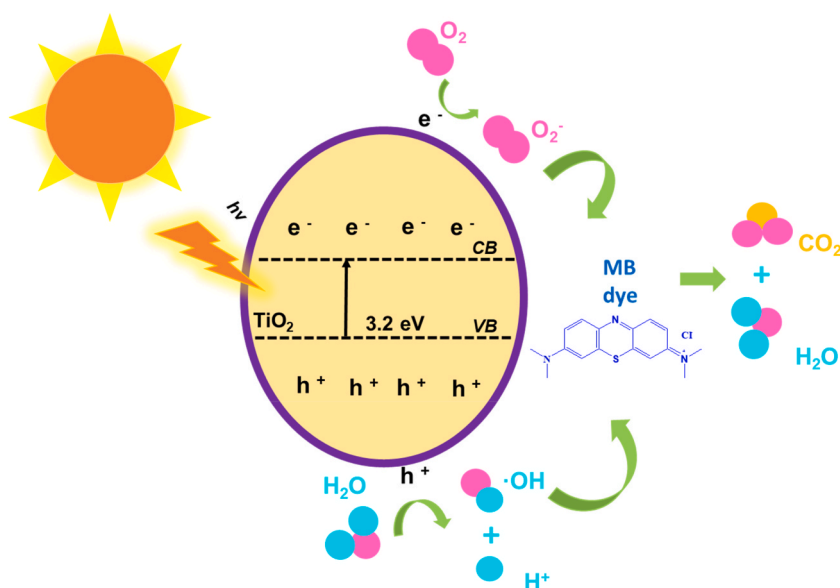

Fig. 8. Mechanism of degradation of MB by TiO_2 [172].

4.3.5. Reduction reaction

In the first reaction, reduction occurs when the excited e^- reduce oxygen (O_2) to form the superoxide radicals ($\bullet O_2^{2-}$) as illustrated in **equation (2)** [174].

$$e_{CB}^- - + O_2 \rightarrow \; \cdot O_2^{2-} \tag{2}$$

4.3.6. Oxidation reaction

In the second reaction, the h^+ oxidise water (H_2O) to produce hydroxyl radicals ($\bullet OH$) as shown in **equation (3)** [174].

$$h_{VB}^+ + H_2O \rightarrow \cdot \cdot OH + H^+ \tag{3}$$

4.3.7. MB dye degradation

The two ROS, superoxide radicals ($\bullet O_2^{2-}$) and hydroxyl radicals ($\bullet OH$) are strong oxidizing agents that break the MB dye molecules into smaller fragments. These fragments are further decomposed into less harmful substances like carbon dioxide (CO_2), water (H_2O) and other inorganic ions (**equation (4)**).

$$\cdot O_2^{2-} + \cdot OH + MB \; Dye \rightarrow CO_2 + H_2O + degraded \; products \tag{4}$$

4.3.8. Mineralization

These processes will repeat until the dye is fully broken down into inorganic compounds, ensuring complete degradation and minimising environmental impact [172]. In summary, when a semiconductor photocatalyst is exposed to light, it undergoes two simultaneous reactions (Fig. 8). The first process includes oxidation (photogenerated holes), whereas the second involves reduction (photogenerated electrons) [173]. However, following absorption of light of the right wavelength, these electrons get excited and transition to the CB, resulting in the formation of a positive hole (h^+) in the VB and a negative electron (e^-) in the CB [174,172].

Numerous photocatalysts have been explored for water treatment, including V_2O_5, TiO_2, Fe_2O_3, ZnO, ZrO_2, WO_3, ZnS, Nb_2O_5, and CdS [146,149]. Among these, ZnO and TiO_2 have attracted considerable attention [171,175–177]. TiO_2 is cost-effective, easily synthesized, and capable of degrading various organic compounds, including dyes [178,179]. On the other hand, ZnO is favoured for its stability and high sensitivity to light when it comes to breaking down organic contaminants [180,181]. These photocatalysts have outstanding chemical and physical properties suitable for the photocatalytic degradation process.

Various studies (Table 3) have been conducted where photocatalysis was used as a primary method to treat dye-contaminated water. Table 3 summarises the findings of these studies where TiO_2 and ZnO nanoparticles as photocatalysts for the degradation of textile dyes. The table includes information on the photocatalyst dosage, dye used, volume of the solution, duration of exposure, and

Table 3
Degradation of dyes by using titanium dioxide (TiO_2) and zinc oxide (ZnO) nanoparticles.

Photocatalyst	Dosage	Dye	Volume (mL)	Time (mins)	%Degradation	Ref
TiO₂	32 mg	TB	20	180	10 %	[182]
		RB	20		20 %	
	0.5 mg	CBBR	100	120	91%-	[183]
	30 mg	MB	300	120	65 %	[176]
	10 mg/L	MB	–	60	96 %	[184]
		RhB			97 %	
	0.1 g	MB	100	300	35,66 %	[185]
		RhB	100		100 %	
	5 g/L	AB10b	–	300	100 %	[186]
	0.30 mg	MB	50	60	96 %	[187]
	37.5 mg	CR	25	50	92.7 %	[188]
		MO		15	97.9 %	
		DR23		60	97.6 %	
	2 g/L	AC113	–	80	94.43 %	[189]
	0.1 g	RhB	30	150	~94 %	[190]
	20 mg	MB	250	180	85 %	[191]
ZnO	200 mg	MB	–	120	64 %	[192]
	0.4 g	MB	400	120	58 %	[193]
		EY			39 %	
	0.05 g	ECBT	100	180	88 %	[194]
	0.2 g	RhB	100	160	95.41 %	[195]
	1 g/L	MB.	–	180	86 %	[196]
	200 mg	BR51	100	330	89.01 %	[197]
	15 mg	MB	15	300	92 %	[198]
		ECBT			86 %	
	15 mg	MB	100	100	~99 %	[199]
		MY			~97 %	
	50 mg	CR	100	180	93 %	[200]
	10 mg	MB	100	60	93 %	[201]

the percentage of dye degradation achieved in each study.

Key findings reported from Kumar et al. [182], showed that under specific conditions the degradation rates for TB and RB were 10 % and 20 %, respectively. The process followed first-order kinetics. Then, Mohamed et al. [183] prepared TiO_2 quantum dots via the sol-gel technique and achieved a photocatalytic efficiency of 91 % when degrading Coomassie brilliant blue R (CBBR) using direct sunlight exposure. Ge et al. [184] synthesized visible-light-responsive TiO_2 using a solvothermal process. The TiO_2 showed excellent photocatalytic capabilities in degrading rhodamine B (RhB) and methylene blue (MB), with over 95 % efficiency under visible light within 60 min. Li et al. [185] synthesized TiO_2 nanoparticles using a hydrothermal approach for photodegradation studies of both RhB and MB. The degradation efficiency of RhB and MB after 300 min was 34 % and 100 %, respectively. Aboul-Gheit et al. [186] synthesized TiO_2 that degraded 100 % of amido black 10b (AB10b) dye after 300 min of illumination. Green synthesis methods by Pavithra et al. [187] achieved 96 % degradation of MB in 1 h, while Bopape et al. [172] reported 65 % degradation of MB in 2 h using TiO_2 nanoparticles. Tatarchuck et al. [188] studied the degradation of Methyl Orange (MO), Congo Red (CR) and Direct Red 23 (DR23) dyes by TiO_2 in water, achieving efficiencies of approximately 98 %, 93 %, and 98 %, respectively. Acid Blue 113 (AB113) was degraded by environmentally synthesized TiO_2 nanoparticles [189], achieving a 94.43 % degradation within 80 min, following pseudo-first-order reaction kinetics. Dodoo-Arhin et al. [190] prepared TiO_2 nanostructures and achieved approximately 94 % degradation of RhB dye under UV light. Ngoepe et al. [191] achieved an 85 % degradation of MB using green-synthesized TiO_2 nanoparticles.

Various studies where zinc oxide (ZnO) photocatalysts were utilised for the degradation of different dyes were also reported in Table 3.

Xue et al. [192] used ZnO nanowires to break down Methylene Blue (MB) dye, achieving a 64 % reduction in MB concentration within 2 h. In their study. Chakrabarti and Dutta [193] investigated the ZnO as an effective catalyst for the photodegradation of MB and Eosin Y (EY) dyes, resulting in a 58 % degradation of MB and a 39 % degradation of EY concentrations using a UV light. Kazeminezhad et al. [194] prepared ZnO nanoparticles using the co-precipitation technique and successfully decomposed 88 % of Eriochrome black-T (EBT) dye. While Dodoo-Arhin et al. [195] utilised nanocrystalline wurtzite ZnO particles as photocatalysts for RhB dye degradation under UV light. They achieved a 95.41 % degradation efficiency under specific conditions. Isai and Shrivastava [196] found their synthesized ZnO efficient against 86 % of MB dye while considering various factors like pH, dye concentration, contact duration, and catalyst amount. While Yashni et al. [197] explored the use of ZnO nanoparticles for degrading Basic Red (BR51) dye. They achieved the highest degradation rate of 89.01 % with specific conditions. Golmohammadi et al. [198] biosynthesised ZnO
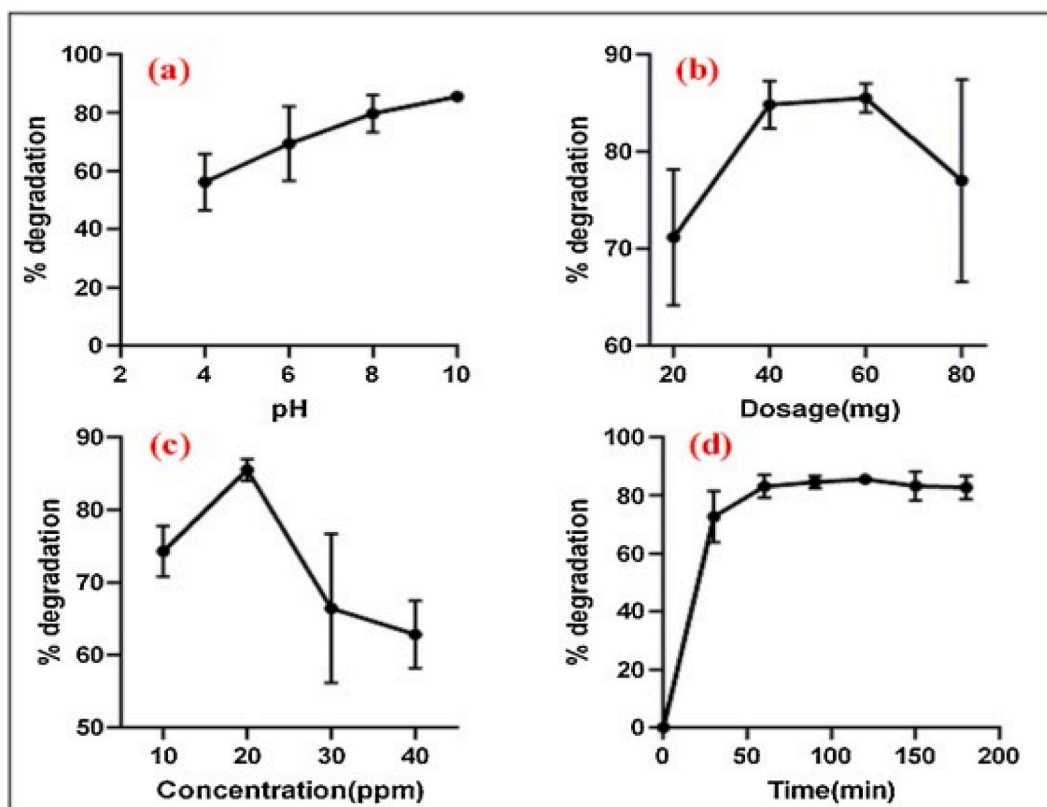

Fig. 9. Photodegradation curves of MB by TiO_2 reporting on on various conditions (a–d). Adapted from Ngoepe et al. [191] with licence number 5837050267115.

nanoparticles and demonstrated their effectiveness in degrading both MB and ECBT dyes under direct solar light, achieving degradation rates of approximately 92 % and 86 %, respectively. The ZnO nanocrystals fabricated by Priyadharshni et al. [199] using coconut husk extract and achieved remarkable photocatalytic capabilities, leading to the degradation of MB (99 %) and metanil yellow (97 %) dyes. While the biosynthesised ZnO-NPs prepared by Chakraborty et al. [175] achieved the highest degradation efficiency of 93 %. Finally, Ameen et al. [200] green synthesized ZnO nanoparticles and demonstrated their ability to degradation ~93 % of methylene blue dye. These studies show the effectiveness of both TiO_2 and ZnO photocatalysts for removal of dyes. However, these two photocatalyst possess differences in photocatalytic activity, stability, and cost. According to studies conducted by AlMohamadi et al. [202], Lin et al. [203], Park et al. [204] and Gelashvili et al. [205] ZnO shows higher photocatalytic activity than TiO_2 this is due to its superior electron mobility and larger surface area. In terms of stability, the TiO_2 showed more stability over multiple cycles while maintaining its photocatalytic efficiency, while ZnO was reported to be less stable with each cycle [202,204]. According to AlMohamadi et al. [202] and Yunus et al. [206], ZnO is more cost-effective compared to ZnO as it is easy to prepare.in contrast, Lin et al. [203] reported TiO_2 to be more cost-effective due to its availability and cheap productions as compared to ZnO. The choice between TiO_2 and ZnO is dependent on specific application requirements. And also, it is important to note that there are numerous parameters that affect the photodegradation process using both TiO_2 and ZnO.

4.3.9. Factors affecting the photodegradation process

4.3.9.1. Effect of pH. The pH of the solution impacts both the adsorption capacity and the charge properties of the photocatalyst [196]. It is a critical factor in the photodegradation of textile dyes using ZnO and TiO_2 photocatalyst as it impacts the photodegradation efficiency (Fig. 9a). This parameter is important in the generation of hydroxyl radicals which assist in the photocatalysis reaction [196]. The industrial effluents are often not neutral, making it necessary to consider the pH effect on degradation rates. The effect of pH against the TiO_2 nanoparticles were studies by various researchers and in the research conducted by Tayeb et al. [178], pH studies of MB using the TiO_2 nanospheres were explored. Therefore, the pH of a dye solution impacts the degradation process. The removal percentages were improved with the increase the pH value. The degradation percentages of ~57 %, ~42 %, and ~95 % were achieved at pH levels 7, 1.4, and 12.6, respectively. The basic pH of 12.6 was found to be the optimum pH of the study.

In another study by Kumar et al. [182], the photodegradation studies on Rose Bengal (RB) and Thymol Blue (TB) dyes using TiO_2
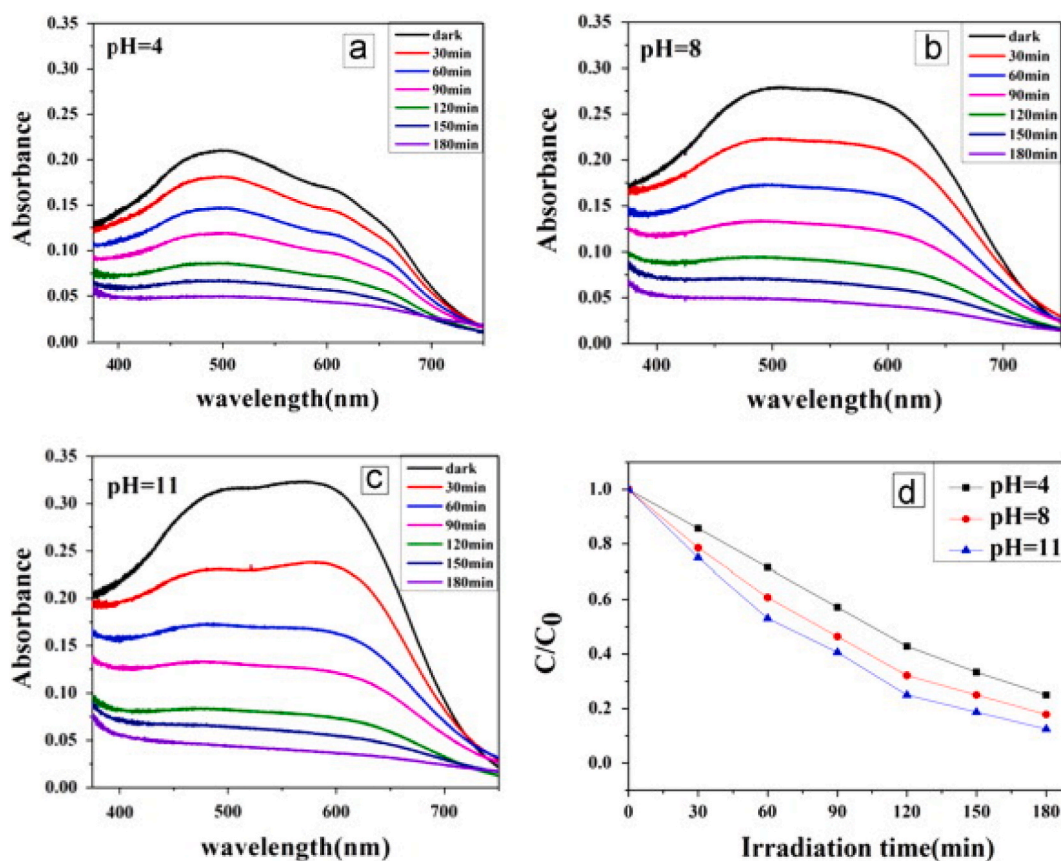

Fig. 10. pH studies on photodegradation of ECB dye by ZnO at pH (a) 4, (b) 8 and (c) 11 and the (d) C/C_0 for pH 4–11. Adapted from Kazeminezhad et al. [194] with licence number 5837800628683.

photocatalyst were conducted. The highest photodegradation efficiency of TB was observed at pH 5–6, with TiO$_2$/PAni/GO achieving degradation efficiency of 96 %. Under basic conditions the TiO$_2$/PAni/GO achieved the photodegradation efficiency of 96 % for the TB dye. The optimal photodegradation for TB occurred within the neutral pH range (6–7), with efficiencies of 98 %, for the TiO$_2$/PAni/GO photocatalyst.

Similarly on the study conducted by Ngoepe et al. [191], explored pH range of 2–10 using the photocatalytic performance of a TiO$_2$ nanocomposite with methylene blue. The results revealed that pH 10 was optimal for effective dye degradation of methyl blue. The highest percentage degradation of ~84.9 % was obtained (Fig. 9a).

For the ZnO semiconductor, experiments were conducted by Chakrabarti et al. [193] using 50 mg/l MB solutions at pH 5.5 to 9.7. It was found that-the efficiency of degradation increased with increasing pH levels. The increase in pH from 5.5 to 9.7 influenced the degradation percentage to rise from 49 % to 62 % within 2 h. Therefore, their optimal pH was found to be 9.7. As observed on Fig. 10a-d, the degradation of ECB dye after 180 min was 75 %, 83 %, and 88 % at pH levels of 4, 8, and 11, respectively. The researchers argued that although maximum degradation occurred at pH 4, ECB dye decomposed more rapidly at pH 11. Therefore, chose pH 11 as the optimum pH.

Isai and Shrivastava [196], studied the pH parameter during the photodegradation process of MB dye within the pH range of 1–10 using a synthesized ZnO and 2%Fe–ZnO. The point of zero charge (pHpzc) of the catalyst was determined to be approximately 8.3 for ZnO and 8.9 for 2%Fe–ZnO. Therefore, doping the ZnO with Fe increased the pHpzc.

In their study, Yashni et al. [197] explored the four pH conditions (3, 5, 9, and 8.15) on the BR51 dye. The maximum degradation of BR51 obtained was ~83 %, ~59 %, ~69 % and 62 % for pH 5, 9, 3 and pH 8.15, respectively. Therefore, the optimal pH was reported to be at pH 5.

Priyadharshini et al. [199], studied the pH parameter on the photodegradation of MB using the ZnO catalyst. As the pH increased to 10, higher degradation performance was observed while the lowest degradation performance was observed at pH of 4. The highest degradation of MB at pH 10 was 99 %. It was concluded that the basic pH generates anions on the catalysts which adsorbs MB resulting in more effective removal of the dye.

The photodegradation of dyes using TiO$_2$ favoured higher basic conditions of pH of 10–12.6 even though various dyes were studied
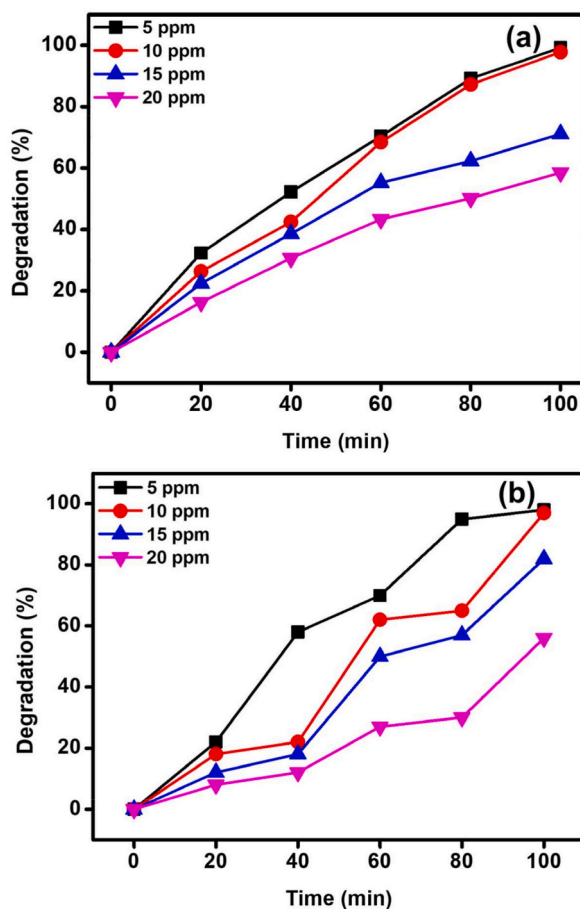

Fig. 11. Effect of (a) MB and (b) MY concentration on the degradation efficiency of the ZnO photocatalyst. Adapted from Priyadharshini et al. [199] with licence CC BY.

[178,191]. An exception is observed on the TiO$_2$/PANi/GO nanocomposite as the optimum pH for the studies were 5–7 for RB and TB dyes. As for the ZnO nanoparticles, the degradation of MB favoured pH of 9.7–10 and for BR51 favoured the pH of 5. These studies highlight the influence of pH on the photodegradation dyes by ZnO and TiO$_2$ nanomaterials, emphasizing the need for pH optimization in wastewater treatment.

4.3.9.2. Effect of concentration. The concentration parameter influences the quantity of dye that could be adsorbed on the catalyst [186]. This parameter also influences the light behaviour during the photocatalysis process [194]. As seen on Fig. 11(a–b), the degradation efficiency decreases as the concentration of dye was increased. This is because of the increased number dye molecules being adsorbed on the TiO$_2$ and ZnO catalysts, therefore, reducing the number of photons that reach the catalyst [186].

Alshehri et al. [177], studied the impact of MB concentration on the photocatalysis process. The concentrations ranging from 2.0×10^{-5} to 12.0×10^{-5} M were explored. The results in the study demonstrated that degradation efficiency decreased with increasing MB dye concentration. Therefore, an optimal concentration was determined to be 1.0×10^{-5} M [177].

Kumar et al. [182] studied the impact dye concentrations on photodegradation of TB and RB. The photodegradation efficiencies for the three photocatalysts were decreasing as the TB concentration was increased. Similarly, the RB dye degradation with increasing RB concentration. It was concluded that higher concentrations of TB and RB restrict light penetration through the dye photocatalyst surface [182].

The dye concentration studies by Ngoepe et al. [191], revealed that at higher concentrations (30 and 40 ppm), the degradation percentages were 66.4 % and 62.8 %, respectively. In contrast, lower concentrations (10 and 20 ppm) showed higher degradation rates of 74.3 % and 85.5 %, respectively (see Fig. 9c). Specifically, the degradation efficiency decreased from 85.5 % at 20 ppm to 62.8 % at 40 ppm [191].

Kazeminezhad et al. [194], study highlights the impact dye concentration of the MB dye on photocatalytic degradation from 25 to 100 mg/L. Similarly, there was a decrease in photocatalytic percentage as the concentration of MB increased [194].

While Yashni et al. [197], showed that the degradation of BR51 was decreasing from 1, 5, and 10 ppm. This reduction in degradation was associated with the diminished penetration of UV light. The higher concentrations of BR51 block the photons from reaching
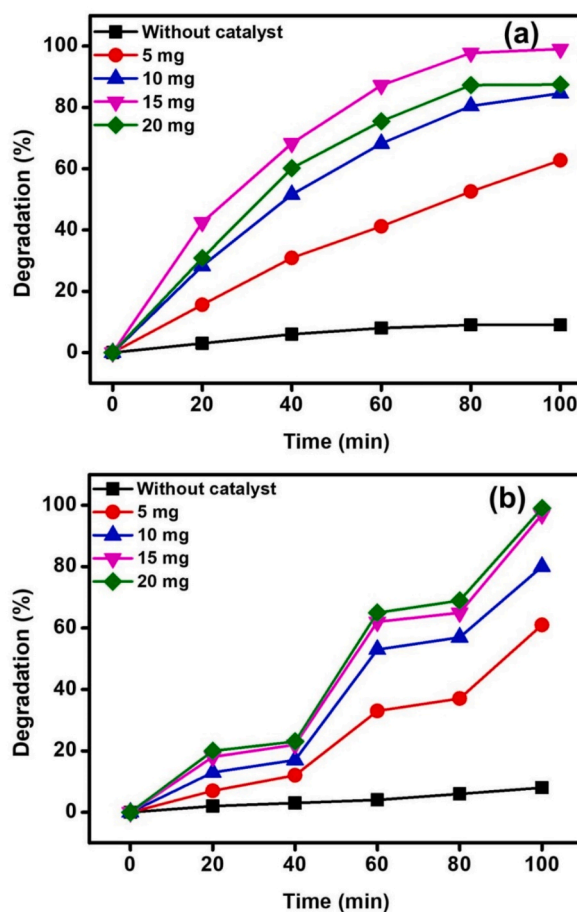

Fig. 12. Effect of photocatalyst loading on the photodegradation of (a) MB and (b) MY by ZnO nanocrystals. Adapted from Priyadharshini et al. [199] with licence CC BY.

the surface of ZnO nanoparticles. Therefore, fewer hydroxyl radicals are available to attack the compound, and the scarcity of active sites on the ZnO nanoparticles further hinders oxidant generation, leading to a reduced degradation rate of BR51 [197].

Fig. 11a-b, compares the degradation efficiency of ZnO photocatalyst against various concentrations of MB and MB dye [199]. As expected, the efficiency of the ZnO nanoparticles decreased with increased dye concentration and the optimum dye concentration was found at 5 ppm. The decrease in degradation of 99 %–58 % was reported on MB and MY degradation decreased from 97 % to 56 % [176]. They associated this reduction with insufficient light absorption on the ZnO surface and lower OH• radicals' production essential for the photodegradation process [194].

As a result, it is critical to maintain an appropriate ratio of photocatalyst to dye concentrations. The findings of concentration investigations of ZnO and TiO$_2$ degradations show that the catalyst works at dye concentrations from 5 ppm to 25 ppm. As a result, photocatalysts were most efficient at dye degradation up to 25 ppm (for MB, RB, and TB) and 10 ppm (for MY and BR51) [177,182,191, 197,199].

4.3.9.3. Effect of photocatalyst dose. The quantity of the catalyst used is another essential parameter influencing the dye degradation process [177]. This parameter also depends on the reaction container size, as increased particle density can lead to more collisions, blocking light from reaching the catalyst particles and reducing hydroxyl radical generation [177]. In addition, some textile dyes can be degraded by UV irradiation only, so it is important to determine the extent of dye photolysis without a catalyst [193]. This process is useful to determine the minimum photocatalyst required to achieve maximum dye decolourization. In their study Chakrabarti et al. [193], started by performing blank experiments for Eosin Y dye without a catalyst to assess photolysis. Then experiments were conducted with varying amounts of ZnO photocatalyst. The photolysis of Eosin Y reached 4 % after 120 min. However, with increasing dose from 0.2 to 1.0 g in 400 ml, the percentage of dye degraded rose from 47 % to 74 % after 2 h. Beyond this, the degradation percentage decreased. Thus, the optimal ZnO dosage for EY degradation was 1.0 g.

The impact of varying the amount of ZnO nanocatalyst was studied by Alshehri et al. [177]. In their experiments, the catalyst load ranged from 5.0 to 30.0 mg/L. There was an increase in degradation rate as the ZnO photocatalyst dose increased up to 25 mg, beyond this photocatalyst dose led to decreased degradation. This is because higher amounts of catalyst result in more dye molecules adsorbing ZnO surface, increasing the hydroxyl radical production, thereby enhancing photocatalytic activity. However, excessive catalyst loading can cause agglomeration of ZnO particles, unfavourable light scattering, and hindered light penetration, reducing photo-degradation efficiency. Therefore, optimising the catalyst concentration is essential for effective photon absorption and to avoid excessive usage of the catalyst. For maximum photocatalytic performance, a ZnO catalyst dose of 25 mg was used in the experiments [177].

The effect of ZnO nanocrystals dosage on the degradation of MB and MY (Fig. 12a-b) was studied by Priyadharshini et al. [199]. The study found that an increase of 5–15 mg ZnO dose led to MB degradation of 63 %–99 % and MY degradation of 61 %–97 %. This was associated with availability of more active sites. However, increasing the dose to 20 mg reduced the degradation to 88 % for MB and 99 % for MY. Higher dosages of ZnO nanocrystals led to agglomeration and aggregations of catalyst which reduced the system's degradation efficiency. The optimal photocatalyst amount of 15 mg was chosen for proceeding studies.

Ngoepe et al. [191] explored the effect of TiO$_2$ dosage on the degradation of MB and dosage amounts ranging from 20 to 80 mg at pH 10 were examined. As shown in Fig. 9b, the degradation percentage increased from 71.2 % at 20 mg to 85.5 % at 60 mg, but then decreased to 77.0 % at 80 mg. This decrease at higher dosages could be attributed to nanoparticle agglomeration. Therefore, excessive amounts of TiO$_2$ nanoparticles can also lead to suspension in the solution [191].

When Isai and Shrivastava [196] examined the impact of photocatalyst loading of 0.2 g–2 g on MB dye degradation, they found that the degradation efficiency increased rapidly with the increase in catalyst concentration but decreased at 2 g due to increased particle-particle interactions and agglomeration. This reduced light absorption by the photocatalyst and prevented interactions with the surface of the catalyst, resulting in fewer excited particles and electron/hole pairs and hydroxyl radicals being produced [191,197]. Therefore, optimum dose was taken to be 1.8 g for both photocatalysts.

Yashi et al. [197] explored the degradation of 1 ppm BR51 at a neutral pH of 7 using ZnO NP doses of 50–200 mg. The degradation percentage increased with higher concentrations, reaching 74.48 % at 100 mg. However, further increases to 150 and 200 mg decreased the degradation rate of BR51 dye. This reduction may be due to reduced sunlight penetration, agglomeration and aggregation of the catalyst, and collisions between activated and ground state molecules controlling the reaction.

These studies have shown that the effectiveness photocatalysis process is affected by the quantity of the catalyst used [191]. Optimal catalyst loading enhances degradation efficiency by increasing active sites and hydroxyl radical production [177,199]. However, excessive catalyst amounts can lead to agglomeration, blocking light penetration and the reduction of catalyst efficiency [196,197]. It is also important to consider the extent of dye photolysis without a catalyst to understand the contribution of direct photolysis to overall degradation [193,199]. Various studies demonstrate that while initial increases in catalyst loading improve degradation rates, beyond a certain point, additional catalyst leads to decreased performance due to aggregation and light scattering [177,191,193,196,197]. Therefore, determining the optimal catalyst concentration is crucial for maximizing photocatalytic efficiency.

4.3.9.4. Effect of time. Time is another aspect that influences photocatalyst performance; ideally, the photocatalysis process should be highly rapid and efficient [143].

Table 3 presents data on various photocatalysts, their dosages, dye types, experimental volumes, degradation times, and the percentage of dye degradation achieved. Interestingly, the degradation time ranges from 15 min to 330 min, and the percentage degradation varies from 10 % to 100 %. The TiO$_2$ degradation percentages vary widely based on dye type, dosage, and experimental

conditions [182–200]. Higher percentages are seen with RhB [185] under certain conditions, while lower percentages are seen with TB [182]. On the contrary, ZnO shows a wide range of degradation efficiency, from 39 % to 99 %, with exposure time significantly impacting it [192–201]. Therefore, it important to study the effect of time on the photocatalysis process.

Ngoepe et al. [191] studied the time parameter (Fig. 9d) on their green-synthesized TiO_2 against the MB dye. The degradation percentage increased with longer UV irradiation, but decreased after 2 h, suggesting that the catalysts had reached their maximum degradation capacity [191]. Isai and Shrivastava [196], explored the time parameter on the photocatalytic degradation of MB dye under optimal conditions. They used a fixed ZnO and 2 % Fe-ZnO catalyst at 1 g/L. The results showed that increasing the time of irradiation of the catalyst increased MB dye degradation. The degradation rate was faster from 0 to 140 min due to the availability of many active sites. After 140 min, the system reaches equilibrium, and the degradation rate decreased due to MB dye particles and the catalyst surface repulsions [196]. From the studies, it was evident that the optimum time degradation of MB dyes was 120 min for TiO_2 and 140 min for ZnO photocatalysts.

4.3.9.5. Effect of reusing the photocatalyst. Photocatalysis is an environmentally friendly technology that typically does not generate waste disposal issues, as the catalysts can be reused [172]. The photocatalysts must be reused at best twice without dropping their efficiency [193]. The reusability parameter is crucial as it can help reduce process costs [191]. Hence, it is of high importance to use photocatalysts which are highly reusable. When Bopape et al. [172], conducted the reusability tests of biosynthesised TiO_2-NPs against MB. The degradation efficiency of the dye reduced with each successive cycle. After four cycles, the photocatalytic efficiency of the TiO_2-NPs decreased up to ~30 %.

Alshehri et al. [177], studied the reusability studies of green synthesized ZnO-NPs on MB dye degradations in UV light irradiation. The recovered ZnO photocatalyst was reused four times under the same conditions, and it showed excellent stability and catalytic efficiency [177].

Kumar et al. [182] performed reusability of photocatalysts against RB and TB (Fig. 13a–b). The degradation efficiencies of the recycled photocatalysts for RB and TB declined with each proceeding cycle. This drop in efficiency of the photocatalysts was due to the loss of some active sites [182].

Ngoepe et al. [191], studied the degradation percentage declined starting from the first cycle, indicating an immediate loss in photocatalytic efficiency. The researchers reported that the decline may be attributed to the partial loss of the catalyst during the recovery process [168]. Similarly, Chakrabarti et al. [193] explored the photodegradation performance of two recycled photocatalyst. The RC-1 and RC-2 degraded 21 % and 23 % of EY dye, respectively.

The recyclability of ZnO nanoparticles (NPs) was assessed by Yashni et al. [171]. The degradation efficiencies of BR51 were 86.13 % for the first run, 82.90 % for the second, 71.90 % for the third, and 66.49 % for the fourth run. These results showed a 20 % reduction in photocatalytic degradation performance after four cycles [197].

The reusability of photocatalysts is critical for photocatalytic processes that are both environmentally friendly and economically effective [193]. While materials such as TiO_2 NPs and ZnO NPs lose efficiency with each reuse cycle, they can still be useful after several cycles. After four cycles, TiO_2-NPs lost 29 % of their efficiency [172], but the ZnO-NPs lost 20 % of their efficiency [197]. Choosing highly recyclable photocatalysts reduces performance loss and operating expenses. Despite certain efficiency reductions owing to active site obstruction and catalyst loss during recovery, many photocatalysts have the potential for continued usage.

4.3.9.6. Effect of reactive species. Throughout the degradation process, various species such as holes (h^+), hydroxyl radicals ($\bullet OH$), superoxide radicals ($\bullet O^{2-}$) and electrons (e^-) are produced [150]. To identify the roles of these species, various chemicals like EDTA, tert-butanol, p-benzoquinone (BQ) and $AgNO_3$, were used as scavengers by Bopape et al. [172] in the reaction system as seen on
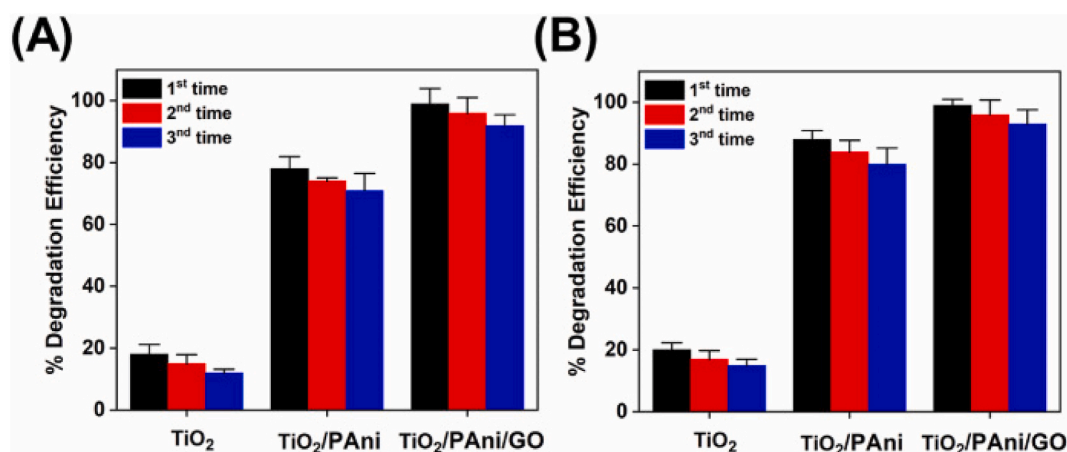

Fig. 13. Reusability studies of (a) thymol blue and (B) Rose Bengal using various photocatalysts. Adapted from Kumar et al. [182] with licence number 5840330370246.
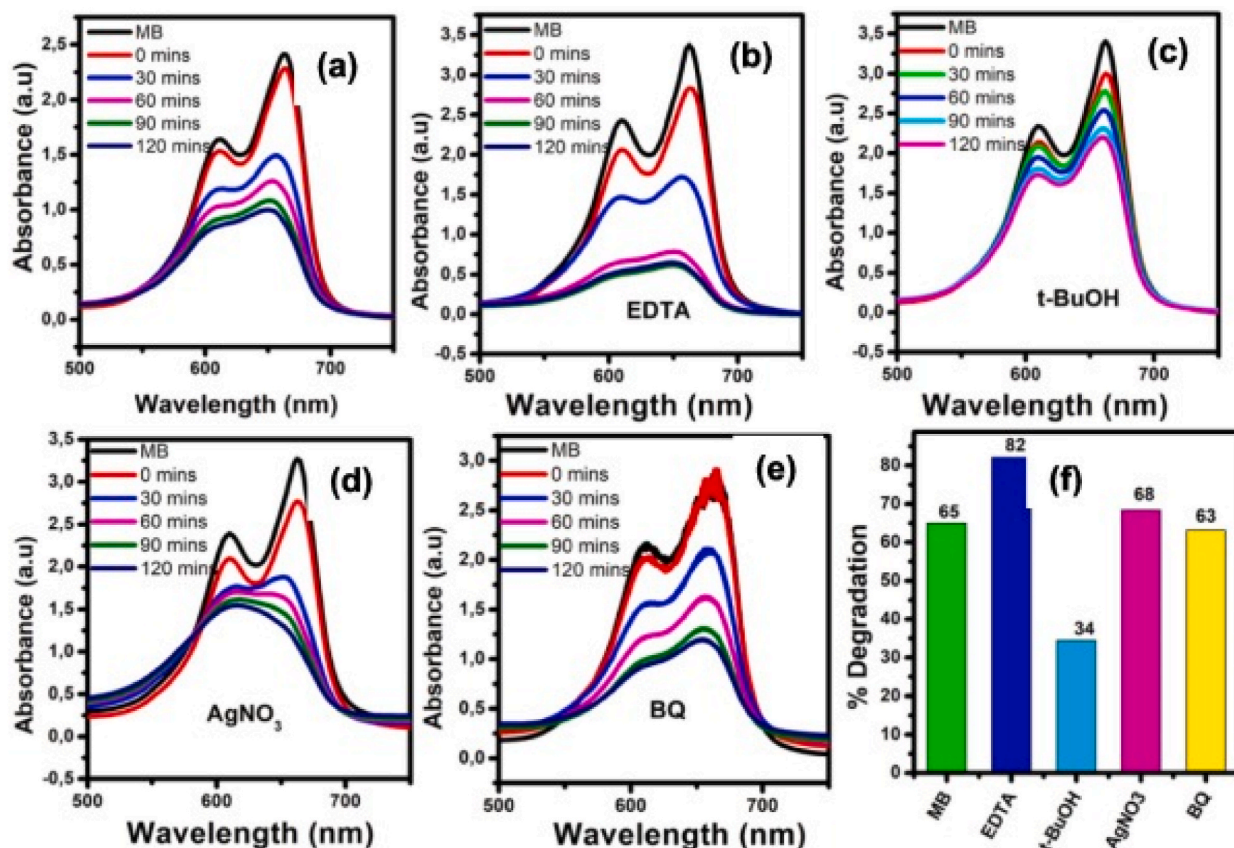
Fig. 14. Degradation graphs of MB by TiO$_2$-NPs with (a) no scavenger, (b) EDTA, (c) t-BuOH, (d) AgNO$_3$, and (e) BQ and (f) Trapping investigations on TiO$_2$-NPs. Adapted from Bopape et al. [172] with licence number 5840360109292.

Fig. 14a-f. The results, shown in Fig. 14a-f, indicate that the addition of EDTA and AgNO$_3$ increased the degradation, suggesting that electrons (e$^-$) and holes (h$^+$) played a lesser role in the degradation compared to other species. On the contrary, the addition of t-BuOH resulted in degradation reduction of 34 %, highlighting that •OH radicals played a major role in the photocatalysis process [172].

Alshehri et al. [177] investigated trapping studies of active species in the photodegradation of MB process. The three scavenger reagents: benzoic acid (BA) for •OH scavenging, benzoquinone (BQ) for •O$_2^{2-}$ scavenging, and ammonium oxalate (AO) for scavenging holes (h$^+$) were used. The addition of benzoic acid significantly reduced the photocatalytic degradation of MB, demonstrating that hydroxyl radicals (•OH) were predominantly responsible for degradation under UV light [177].

In their study, Quek et al. [181] employed various scavenger agents to trap specific reactive species: benzoquinone (BQ) for superoxide anions (O^{2-}), catalase for hydrogen peroxide (H$_2$O$_2$), EDTA for holes (h$^+$), histidine for singlet oxygen (1O$_2$), and tert-butanol for hydroxyl radicals (•OH). The introduction of these radical scavengers into the photocatalytic system led to a reduction in antibacterial activity, highlighting the importance of each reactive species in the photocatalytic process.

These studies highlight the important roles played by various reactive species during the photodegradation process. Majority of results indicate that hydroxyl radicals (•OH) are the highest contributors to the MB degradation, as evidenced by a substantial decrease in degradation efficiency when hydroxyl radicals were scavenged. In contrast, scavengers targeting other species, such as electrons and holes, had a lesser impact on degradation rates [177,181]. The reduction in photocatalytic activity upon scavenging these species emphasizes their importance in achieving effective degradation and antibacterial performance, respectively. Therefore, understanding the roles of these reactive species is vital for optimising photocatalytic systems and enhancing their efficiency dye degradation applications.

4.3.9.7. Effect of light. While studies have shown that TiO$_2$ and ZnO are efficient, it is important to note that both photocatalysts have numerous limitations [171,175]. These include high recombination rates, small surface areas, and large bandgaps [171]. TiO$_2$ has been reported to have a bandgap of around 3.2 eV, while ZnO has a bandgap of ~3.4 eV [175]. The effect of light parameter on the photocatalytic process was studied by various researchers.

Alshehri et al. [177] employed the green synthesized ZnO-NPs as a photocatalyst for degrading MB dye under a UV light source and a maximum of 88.4 %. While Bopape et al. [172], obtained the photodegradation efficiency of 65 % on MB dye utilising the bio-synthesised 30 g TiO$_2$-NPs under UV light. Similarly, utilising the UV light irradiation Ngoepe et al. [191] achieved photocatalytic

degradation ~86 % of MB using their green synthesized TiO$_2$ photocatalyst. Tayeb et al. [178], also used UV light irradiation and degraded 97.6 % of MB dye using TiO$_2$ nanoparticles. While Li et al. [185] found that the prepared ZnO exhibited more than 30X degradation efficiency against dyes than the P25 under both UV and UV–vis irradiation. Furthermore, these photocatalysts achieved higher photocatalytic efficiency under UV light than UV–vis light. Kumar et al. [182], utilised the visible light source to study photocatalytic degradation of TB and RB dyes. The maximum degradation levels for TB and RB were between 85 and 99 %, utilising
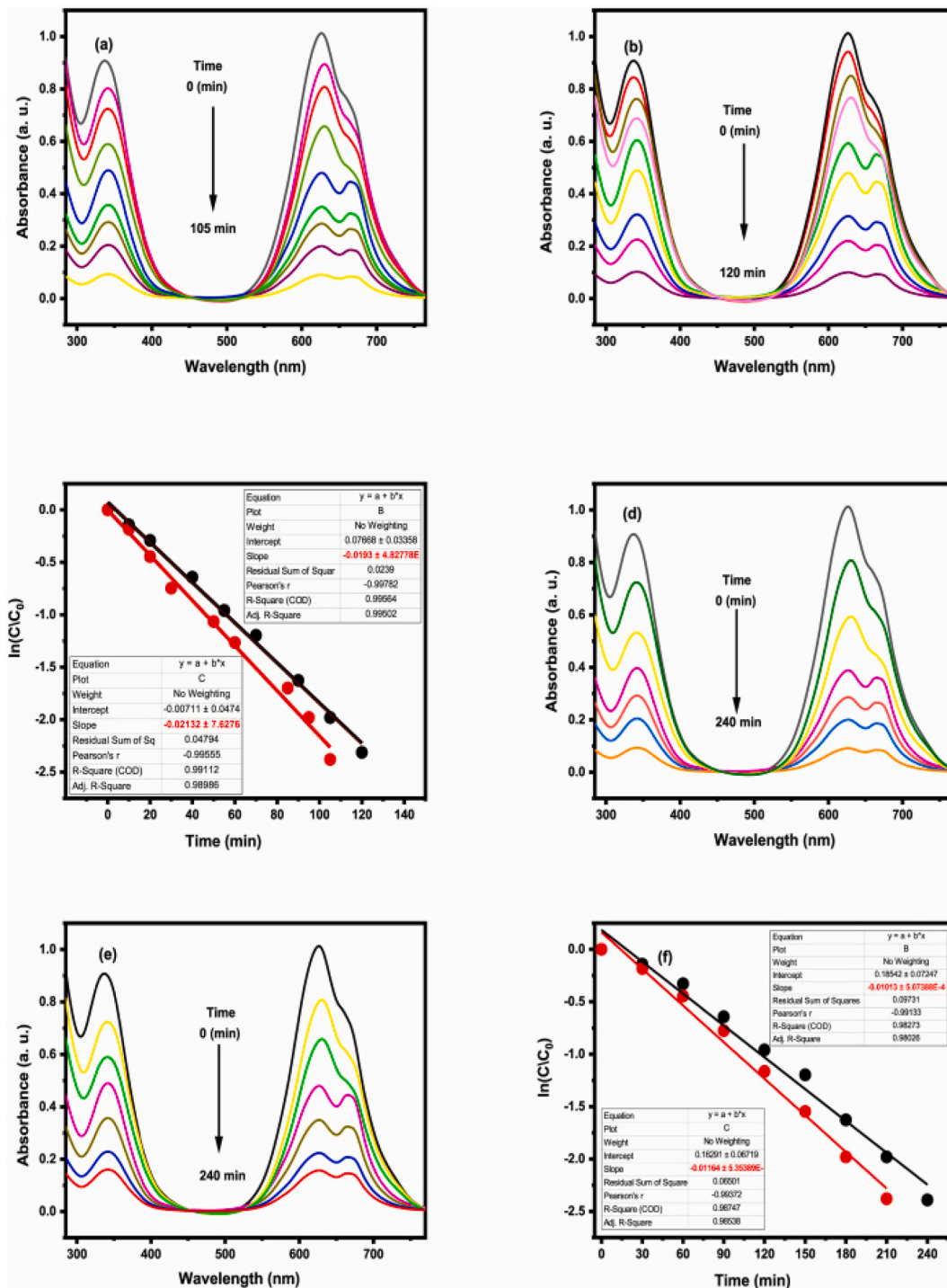

Fig. 15. Photodegradation spectra and kinetics plots of CBBR dye photodegradation rates in the presence of different TDs, measured using the UV–vis light (a–c) and solar light (d–f). Adapted from Mohamed et al. [183] with license number 5840430324890.

TiO_2/PAni/GO photocatalyst.

A study by Mohamed et al. [183], compared the photocatalytic efficiencies of TiO_2 quantum dots (TDs) against Coomassie brilliant blue R (CBBR) under direct solar and UV–vis light irradiation (Fig. 15). The photocatalytic degradation of CBBR under solar and UV–vis irradiation light were 91 % (after 240 min) and 89 % (after 120 min), respectively [183]. These results indicate that the TDs can be used under direct sunlight which is a cheaper and more sustainable process that could be easily implemented in the existing water treatment processes. In another study, Ge et al. [184] synthesized visible-light active TiO_2 photocatalysts. The results demonstrated effective photocatalytic performance of TiO_2 against the MB and RhB. For RhB and MB, the photodegradation efficiency was reported to be >95 % in 60 min of visible light exposure. While the Pavithra et al. [164], prepared *C. gigantean* leaf-assisted TiO_2 NPs which degraded 96 % MB in 60 min under direct sunlight exposure.

The use of ZnO nanoparticles as a photocatalyst in the degradation of RhB dye under UV light was investigated by Dodoo-Arhin et al. [195], and the maximum degradation efficiency of ~95.41 % was reported. Finally, Golmohammadi et al. [198], prepared ZnO NPs that were utilised to degrade two (MB and ECBT) in direct sunlight. The ZnO NPs showed excellent photocatalytic activity, achieving 92 % and 86 % degradation efficiencies within 5 h for MB and ECBT, respectively.

These studies show that the photocatalytic ability of both TiO_2 and ZnO is light dependent. Although, TiO_2 and ZnO are well-known for their photocatalytic properties, they have high recombination rates, small surface areas, and wide bandgaps (3.2 eV for TiO_2 and 3.37 eV for ZnO), which limit visible light absorption [171,175]. These limitations indicate that, while efficient, their preparation and implementation should be improved.

Several investigations have highlighted the performance of TiO_2 and ZnO under UV radiation, with ZnO nanoparticles showing high degradation efficiency of MB dye, reaching up to 88.4 % [154]. While, the TiO_2 nanoparticles have shown varying degradation efficiencies for MB dye under UV radiation, ranging from 65 % [172] to 86 % [191] and even 97.6 % [178]. Microscale ZnO had better photocatalytic activity than Degussa P25 TiO_2 under UV–visible and visible irradiation [182], demonstrating that size and shape may affect performance.

Studies on photocatalytic activity under visible light have yielded mixed results. TiO_2/PAni/GO, TiO_2/PAni, and TiO_2 catalysts achieved degradation levels of 85–99 % for Thymol Blue and 60–97 % for Rose Bengal, indicating that visible light can be effective, but with varying degrees of success [182]. *C. gigantean* leaf-assisted TiO_2 NPs degraded MB by 96 % in 60 min under direct sunshine, indicating a sustainable strategy to solar utilisation [187]. Therefore, photocatalysts based on direct sunshine and visible light show great promise for long-term usage. TiO_2 quantum dots and *C. gigantean* leaf-assisted TiO_2 NPs degrade effectively in sunlight, providing a cost-effective and ecologically beneficial solution for water treatment [183,187]. While the ZnO nanoparticles have also demonstrated outstanding photocatalytic efficacy in sunshine, with MB and ECBT breakdown rates of 92 % and 86 %, respectively, within 5 h [198]. Although TiO_2 and ZnO are efficient photocatalysts, their efficacy is affected by light conditions and intrinsic limits. Advances in photocatalyst design, such as optimising particle size and investigating visible light activity, can improve their practical applicability. Furthermore, using direct sunshine or visible light is a more sustainable and cost-effective method for photocatalytic processes.

5. Application of photocatalysis as an industrial treatment method for textile effluents

The increasing production of harmful textile dye-contaminated wastewater remains a critical environmental issue [198–207]. This presents a considerable obstacle to traditional water treatment systems currently in place [196]. Thus, researchers have explored a variety of chemical, physical and biological treatment methods, with their effectiveness varying depending on the specific conditions of the experiments [195]. The discharge of dye effluents directly into natural water streams is hazardous to aquatic ecosystems' photosynthetic activities [207,208]. As a result, these effluents not only harm the environment, but also represent a risk to human health via the food chain [180]. This is due to the presence of metals and aromatic compounds in textile effluents, which cause mutagenic or teratogenic effects on aquatic creatures [207].

Moreover, in many instances, organic substances like dyes in various water sources resist degradation by pre-treatment methods, leading to the generation of harmful disinfection by-products that may pose health risks [208–210]. Dye molecules exhibit a higher degree of complexity as they consist of multiple aromatic rings interconnected in a fully conjugated arrangement [211]. Therefore, not only is it expensive for wastewater treatment plants to treat the dye effluents from textile industries, but it is also harmful to the environment and humans at large [212]. It is highly advisable for textile industries to select a suitable treatment method for the dye effluents before discarding into natural water streams.

A successful treatment of textile wastewater can be described as a procedure that eliminates or lowers the concentrations of significant physico-chemical characteristics of dyes before its ultimate disposal [213]. Therefore, literature have shown that the use of

Table 4
Studies showing photocatalysis as a treatment method for various industrial effluents.

Pre-treatment method	Pollutant	Type of Waste	% Removal	Time (mins)	References
UV/alkaline H_2O_2 pre-treatment (UHP)	sisal waste	Agricultural	76.6 % (delignification)	600	[210]
UV/TiO_2	Total organic carbon (TOC)	Municipal	50 %	360	[213]
TiO_2-biological	Crystal violet (CV)	Industrial	94 %	90	[214]
TiO_2	Carbamazepine (CBZ)	Hospital	78 %	240	[215]
TiO_2/VUV	Oil	Food	70 ± 3 %	10	[180]
TiO_2 P25	Total organic	Petrochemical	99.5 %	360	[216]
TiO_2	COD	Textile and pulp	87 %	300	[217]

photocatalysis emerges as an effective technology for the treatment of dye effluents before they could be released to the environment [189–193]. The successful treatment is dependent on the characteristics of the dye molecule targeted for degradation [205–210]. Utilising photocatalysis as a preliminary treatment process shows promise in addressing limitations associated with traditional methods [188,209]. This method involves improving the degradability of dyes before releasing to the environment as evidenced by studies of the dye-containing wastewater been successfully treated by photocatalysis [182–201].

Additionally, various studies (Table 4) have been conducted where photocatalysis was employed as a preliminary treatment method. Yang et al. [212] research investigated the combined approach of UV photocatalysis and alkaline H_2O_2 pre-treatment (UHP) to improve the subsequent enzymatic hydrolysis of sisal waste, comparing it with alkaline H_2O_2 pre-treatment (AHP). The optimal conditions for UHP were determined to be 0.1 g/g dried sisal waste, pH 10.0, and UV radiation for 6 h, resulting in a delignification rate of 76.6 %, a sugar conversion of 71.2 %, and glucose conversion of 91.6 %.

Ali et al. [213] study examined the effectiveness of a solar photocatalysis reactor in the pre-treatment of wastewater for removal of total organic carbon (TOC) and turbidity. The process involved UV sunlight/TiO_2, UV sunlight and UV sunlight/H_2O_2 nanocatalysts to membrane fouling. The research assessed the impact of time and solar radiation on TOC and turbidity removal. The study found maximum removal efficiencies of 95 % for turbidity and 31 % for TOC at with optimal conditions.

While Chen et al. [214] studied the effectiveness of a combined photocatalytic-biological system in degrading crystal violet (CV) from a water solution was evaluated. Preliminary tests revealed that the optimal operational conditions for the photoreactor included a reaction time of 1.5 h, pH level of 7.0, and a retention time of 2.0 min. Under these specified conditions, the photocatalytic reaction resulted in a 94 % reduction in the toxicity of the CV solution.

Chong et al. [218] explored a wastewater pre-treatment system using titanium dioxide (TiO_2) nanofibers. The goal was to enhance the biodegradability of carbamazepine (CBZ) in synthetic hospital effluent. The data demonstrated that the TiO_2 pre-treatment system, when employed independently, efficiently degraded 78 % of the CBZ drug.
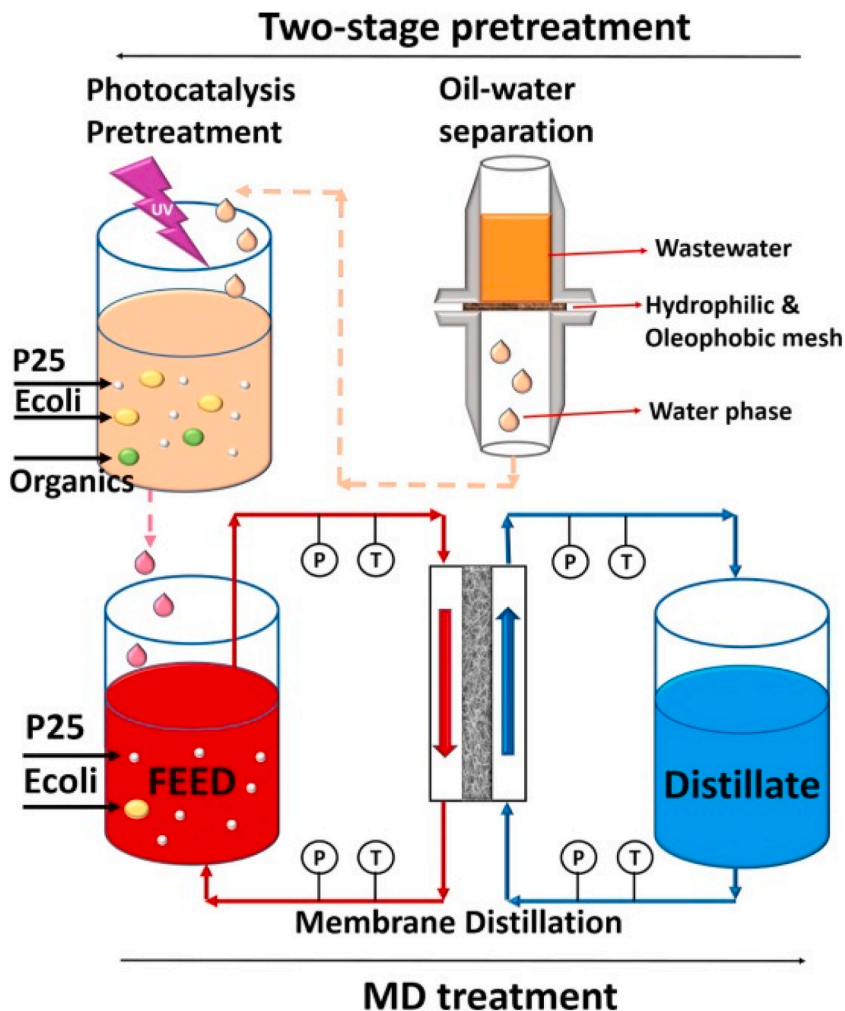

Fig. 16. illustrates a diagram of a laboratory-scale hybrid system featuring a two-stage pre-treatment process. Adapted from Li et al. [185] with license number 5692610107599.

Kang et al. [215], studied the effectiveness of a vacuum ultraviolet (VUV) and TiO$_2$ oxidation system for pre-treatment of oily wastewater from restaurants. Under optimal conditions, the VUV and TiO$_2$/VUV process achieved removal efficiencies of >50 %, and 86 %, respectively.

Li et al. [180], combined membrane distillation and photocatalytic degradation for treating and reusing petrochemical wastewater (Fig. 16). The results showed that the modified stainless-steel mesh/glass microfiber filter removes oil emulsions, and TiO$_2$ P25 serves as the photocatalyst in the photocatalysis phase.

Balcioglu et al. [216] explored the treatability of mixed raw, coagulated, and biologically pre-treated wastewater from textile and pulp sources, as well as effluents from various process stages, was investigated using an enhanced heterogeneous photocatalytic oxidation process. Treatment effectiveness was assessed based on TOC, COD, BOD$_5$, and dye removal. The study found that photocatalytic oxidation treatment with H$_2$O$_2$ was more efficient in removing pollutants from pre-treated wastewater samples. For bio-treated Kraft bleaching and textile effluents, 52 % and 87 % COD removal were achieved, respectively. The addition of ferric ion accelerated the oxidation time but did not impact total COD reduction. Dye removal was achieved within the first hour, but complete decolourization was not achieved for pulp effluents.

The studies presented in Table 4 reported on the utilisation of photocatalysis alone or with other methods as a successful pre-treatment method for various industrial effluents [214,217]. When photocatalysis alone or coupled with various method were employed on industrial effluents, various contaminants were removed to certain levels. In a case of organic contaminants, CV was removed up to 90 % [214], CBZ up to 78 % [215], TOC up to 50 %, *etc.*

Therefore, textile industries generate significant amounts of dye-contaminated wastewater, which poses significant environmental and health risks [172]. Traditional water treatment systems struggle to handle these effluents, which disrupt photosynthetic activity and pose risks to human health through the food chain [196]. These methods are often ineffective in completely degrading or removing dye contaminants, and their excessive cost and environmental impact make them less viable [182]. There is a pressing need for textile industries to handle dye effluents before releasing to wastewater and natural water streams. Additionally, studies have highlighted photocatalysis as a promising technology for treating dye-contaminated wastewater, improving the degradability of dyes and making it a more efficient pre-treatment option [183–201]. Other studies have shown that photocatalysis alone or in combination with other methods (e.g., UV, H$_2$O$_2$) showed promise for treating dye-bearing wastewater [206,217]. Textile should consider adopting photocatalysis as a preliminary treatment method to ease the treatment of dyes by traditional methods. Ensuring that industrial effluents meet acceptable standards before discharge is crucial for environmental protection and public health.

6. Challenges and future prospects

6.1. Photocatalysts and light source

A rapid photodegradation process of dyes by both TiO$_2$ and ZnO requires the use of UV light which is more expensive than the sunlight. Most studies under visible or sunlight reach the highest degradation of dyes after hours of degradation.

It is essential to investigate doping techniques to reduce the band gaps of TiO$_2$ and ZnO, allowing for the utilisation of visible wavelengths. Additionally, retrieving photocatalysts from the slurry following the photodegradation process is not economically practical. While using immobilized catalysts could potentially resolve this challenge, it is crucial to address the preservation of photoactivity in immobilized forms.

6.2. Textile dye effluents

Most studies of degradation of dyes have been investigated under optimized conditions using only one type of dye at the time, while most textile effluents contain a mixture of dyes. Therefore, studies that involve the degradation of a mixture of dyes should be explored to properly record the efficiency of these photocatalysts against an array of dyes.

6.3. By-products of photocatalysis

The by-products of the dyes after going through the photodegradation process and their effect to the environment should be explored in detail.

6.4. Economic implications

The literature reports that the enhanced removal efficiency can be investigated by evaluating a mix of innovative pre-treatment methods. One potential approach involves integrating coagulation/flocculation with photodegradation. This suggestion might be expensive to implement and maintain by textile industries, however a trade-off between cost and efficiency can be considered.

6.5. Regulation of textile dye effluents

Regulative bodies like the Ecological and Toxicological Association of the Dyestuffs Manufacturing Industry (ETAD) work to mitigate the toxic effects of dye products. However, characteristic challenges of dye degradation, such as aromatic structures, high organic content, non-biodegradability, and resistance to light, necessitate urgent attention to eliminate these substances effectively

before reaching natural water streams.

6.6. Treatment of textile dye effluents

Conventional treatment methods for removing textile dyes from water, such as coagulation/flocculation, membrane filtration, ion exchange, and adsorption, have been widely employed but have various limitations.

Photocatalysis is a promising preliminary treatment method for textile dye effluents. The review explores the efficiency of photocatalysis as a treatment of textile effluents. It provided multiple evidence where industries in various sectors have utilised photocatalysis as a pre-treatment method for their effluents before releasing to the environment. Also, the need to address several challenges of photocatalysis, such as the dependence on UV light, investigation of mixed dye effluents, exploration of by-products, and their environmental impact should be explored. Finally, to ensure that textile industries comply, the ETAD should implement severe regulations.

7. Conclusion

The high demand for dyes in the textile industry has led to severe environmental consequences, including water and soil contamination. The use of water and chemicals in textile production results in the generation of sludge and harmful effluents, which pose significant challenges to aquatic life by reducing photosynthesis and dissolved oxygen levels. Textile dye effluents, particularly reactive, sulphur, cationic and anionic types, have diverse applications and are harmful to the environment and aquatic life. Regulative bodies like the Ecological and Toxicological Association of the Dyestuffs Manufacturing Industry (ETAD) work to ease the toxic effects of dye products. However, characteristics of dyes, such as the aromatic structures, high organic content, non-biodegradability, and resistance to light make it difficult to remediate from wastewater. This, therefore, necessitate an urgent technique to successfully remove these substances effectively. Conventional treatment methods for removing textile dyes from water, such as coagulation/flocculation, membrane filtration, ion exchange, and adsorption, have been widely employed but have various limitations such as inefficient removal, high cost, sludge production *etc.*

Advanced oxidation processes (AOPs), such as electrochemical, sonochemical, and photocatalytic methods, have demonstrated remarkable efficacy in treating toxic organic pollutants and emerging contaminants. However, challenges such as dependence on UV light for efficient photodegradation, investigation of mixed dye effluents, exploration of by-products, and their environmental impact need further research.

Photocatalysis, a promising pre-discharge method, employs photocatalysts like TiO_2 and ZnO to break down pollutants using light. The review explores the efficiency of photocatalysis as a pre-discharge treatment of industrial effluents, mainly the textile effluents. It provided multiple evidence where industries in various sectors have utilised photocatalysis as a pre-discharge/pre-treatment method for their effluents before releasing to the environment. Also, the need to address several challenges of photocatalysis, such as the dependence on UV light, investigation of mixed dye effluents, exploration of by-products, and their environmental impact was also highlighted.

CRediT authorship contribution statement

Dineo A. Bopape: Writing – review & editing, Writing – original draft, Resources, Project administration, Methodology, Investigation, Funding acquisition, Formal analysis, Data curation, Conceptualization. **Bulelwa Ntsendwana:** Writing – review & editing, Supervision, Investigation, Conceptualization. **Fumani D. Mabasa:** Writing – review & editing, Supervision, Project administration.

Declaration of competing interest

The authors declare that they have no known competing financial interests or personal relationships that could have appeared to influence the work reported in this paper.

Acknowledgements

References

[1] F.N. Chaudhry, M.F. Malik, Factors affecting water pollution: a review, J. Ecosyst. Ecography 7 (1) (2017) 225–231.
[2] P.K. Goel, Water pollution: causes, effects and control, New age international (2006).
[3] R.P. Schwarzenbach, T. Egli, T.B. Hofstetter, U. Von Gunten, B. Wehrli, Global water pollution and human health, Annu. Rev. Environ. Resour. 35 (2010) 109–136.
[4] A. Inyinbor Adejumoke, O. Adebesin Babatunde, P. Oluyori Abimbola, A. Adelani Akande Tabitha, O. Dada Adewumi, A. Oreofe Toyin, Water pollution: effects, prevention, and climatic impact, Water Challenges of an Urbanizing World 33 (2018) 33–47.
[5] A. Lintern, J.A. Webb, D. Ryu, S. Liu, U. Bende-Michl, D. Waters, P. Leahy, P. Wilson, A.W. Western, Key factors influencing differences in stream water quality across space, Wiley Interdisciplinary Reviews: Water 5 (1) (2018) e1260.

[6] G. Xu, P. Li, K. Lu, Z. Tantai, J. Zhang, Z. Ren, X. Wang, K. Yu, P. Shi, Y. Cheng, Seasonal changes in water quality and its main influencing factors in the Dan River basin, Catena 173 (2019) 131–140.

[7] S. Kurwadkar, S.R. Kanel, A. Nakarmi, Groundwater pollution: occurrence, detection, and remediation of organic and inorganic pollutants, Water Environ. Res. 92 (10) (2020) 1659–1668.

[8] R. Srinivasan, Advances in application of natural clay and its composites in removal of biological, organic, and inorganic contaminants from drinking water, Adv. Mater. Sci. Eng. 2011 (2011).

[9] S. Mishra, A. Maiti, The efficiency of Eichhornia crassipes in the removal of organic and inorganic pollutants from wastewater: a review, Environmental science and pollution research 24 (2017) 7921–7937.

[10] C.A. Basha, E. Chithra, N.K. Sripriyalakshmi, Electro-degradation and biological oxidation of non-biodegradable organic contaminants, Chemical engineering journal 149 (1–3) (2009) 25–34.

[11] M. Arami, N.Y. Limaee, N.M. Mahmoodi, N.S. Tabrizi, Removal of dyes from colored textile wastewater by orange peel adsorbent: equilibrium and kinetic studies, J. Colloid Interface Sci. 288 (2) (2005) 371–376.

[12] A. Rafiq, M. Ikram, S. Ali, F. Niaz, M. Khan, Q. Khan, M. Maqbool, Photocatalytic degradation of dyes using semiconductor photocatalysts to clean industrial water pollution, J. Ind. Eng. Chem. 97 (2021) 111–128.

[13] S. Chabri, A. Dhara, B. Show, D. Adak, A. Sinha, N. Mukherjee, Mesoporous CuO–ZnO p–n heterojunction based nanocomposites with high specific surface area for enhanced photocatalysis and electrochemical sensing, Catal. Sci. Technol. 6 (9) (2016) 3238–3252.

[14] A. Sridhar, M. Ponnuchamy, A. Kapoor, S. Prabhakar, Valorization of food waste as adsorbents for toxic dye removal from contaminated waters: a review, J. Hazard Mater. 424 (2022) 127432–127459.

[15] K. Santhy, P. Selvapathy, Removal of reactive dyes from wastewater by adsorption on coir pith activated carbon, Bioresour. Technol. 97 (11) (2006) 1329–1336.

[16] N. Nooraee Nia, M. Rahmani, M. Kaykhaii, M. Sasani, Evaluation of eucalyptus leaves as an adsorbent for decolourization of methyl violet (2B) dye in contaminated waters: thermodynamic and kinetics model, Modeling Earth Systems and Environment 3 (2) (2017) 825–829.

[17] M.T. Rahaman, A.D. Pranta, M.R. Repon, M.S. Ahmed, T. Islam, Green production and consumption of textiles and apparel: importance, fabrication, challenges and future prospects, Journal of Open Innovation: Technology, Market, and Complexity (2024) 100280.

[18] B. Lellis, C.Z. Fávaro-Polonio, J.A. Pamphile, J.C. Polonio, Effects of textile dyes on health and the environment and bioremediation potential of living organisms, Biotechnology Research and Innovation 3 (2) (2019) 275–290.

[19] G.M. Ratnamala, K.V. Shetty, G. Srinikethan, Removal of remazol brilliant blue dye from dye-contaminated water by adsorption using red mud: equilibrium, kinetic, and thermodynamic studies, Water, Air, Soil Pollut. 223 (9) (2012) 6187–6199.

[20] I. Ahmad, F. Aqil (Eds.), New Strategies Combating Bacterial Infection, John Wiley & Sons, 2008.

[21] S. Kang, Y. Zhao, W. Wang, T. Zhang, T. Chen, H. Yi, F. Rao, S. Song, Removal of methylene blue from water with montmorillonite nanosheets/chitosan hydrogels as adsorbent, Appl. Surf. Sci. 448 (2018) 203–211.

[22] M.T. Uddin, M.A. Islam, S. Mahmud, M. Rukanuzzaman, Adsorptive removal of methylene blue by tea waste, J. Hazard Mater. 164 (1) (2009) 53–60.

[23] T. Islam, M.R. Repon, T. Islam, Z. Sarwar, M.M. Rahman, Impact of textile dyes on health and ecosystem: a review of structure, causes, and potential solutions, Environ. Sci. Pollut. Control Ser. 30 (4) (2023) 9207–9242.

[24] M.T. Islam, N.B. Rafique, M. Mou, D. Roy, R.S. Sadi, Z.C. Das, A.K. Talukder, M. Ahmed, M.M. Rahman, M.G. Haider, Textile dyeing wastewater negatively influences the hematological profile and reproductive health of male Swiss albino mice, Asian Pacific Journal of Reproduction 13 (4) (2024) 169–177.

[25] S.R. Mustafa, A.A. Hadeer, V. Ali, S.A. Hakeem Ali, Study pathological changes to evaluate efficient treatment of industrial dyes in wastewater, Revis Bionatura 8 (3) (2023) 97.

[26] S. Dutta, S. Adhikary, S. Bhattacharya, D. Roy, S. Chatterjee, A. Chakraborty, D. Banerjee, A. Ganguly, S. Nanda, P. Rajak, Contamination of textile dyes in aquatic environment: adverse impacts on aquatic ecosystem and human health, and its management using bioremediation, J. Environ. Manag. 353 (2024) 120103.

[27] F. Bu, B. Gao, Q. Yue, C. Liu, W. Wang, X. Shen, The combination of coagulation and adsorption for controlling ultra-filtration membrane fouling in water treatment, Water 11 (1) (2019) 90.

[28] I. Khouni, G. Louhichi, A. Ghrabi, P. Moulin, Efficiency of a coagulation/flocculation–membrane filtration hybrid process for the treatment of vegetable oil refinery wastewater for safe reuse and recovery, Process Saf. Environ. Protect. 135 (2020) 323–341.

[29] S.I. Sim, Y.H. Teow, Integrated Membrane-adsorption system as a sustainable development approach for semiconductor-industry wastewater treatment, Mater. Today: Proc. (2023).

[30] S.B. Madduri, R.R. Kommalapati, Photocatalytic degradation of azo dyes in aqueous solution using TiO2 doped with rGO/CdS under UV irradiation, Processes 12 (7) (2024) 1455.

[31] S. Ramola, D. Pandey, S. Joshi, N. Rawat, Role of biochar supported nano-photocatalysts for removal of dyes, in: Biochar-Based Nanocomposites for Contaminant Management: Synthesis, Contaminants Removal, and Environmental Sustainability, Springer International Publishing, Cham, 2023, pp. 93–105.

[32] R. Gaur, J. Patel, S. Shahabuddin, Photocatalysis as an effective and sustainable approach for environmental remediation, in: Sustainable Technologies for Remediation of Emerging Pollutants from Aqueous Environment, Elsevier, 2024, pp. 411–429.

[33] S. Sagadevan, I. Fatimah, T.C. Egbosiuba, S.F. Alshahateet, J.A. Lett, G.K. Weldegebrieal, M.V. Le, M.R. Johan, Photocatalytic efficiency of titanium dioxide for dyes and heavy metals removal from wastewater, Bull. Chem. React. Eng. Catal. 17 (2) (2022) 430–450.

[34] J. Sharma, S. Sharma, V. Soni, Classification and impact of synthetic textile dyes on Aquatic Flora: a review, Regional Studies in Marine Science 45 (2021) 101802.

[35] A. Makofane, D.E. Motaung, N.C. Hintsho-Mbita, Photocatalytic degradation of methylene blue and sulfisoxazole from water using biosynthesized zinc ferrite nanoparticles, Ceram. Int. 47 (16) (2021) 22615–22626.

[36] L.M. Mahlaule-Glory, S. Mapetla, A. Makofane, M.M. Mathipa, N.C. Hintsho-Mbita, Biosynthesis of iron oxide nanoparticles for the degradation of methylene blue dye, sulfisoxazole antibiotic and removal of bacteria from real water, Heliyon 8 (9) (2022) e10536.

[37] S. Munyai, L.M. Mahlaule-Glory, N.C. Hintsho-Mbita, Green synthesis of Zinc sulphide (ZnS) nanostructures using S. frutescences plant extract for photocatalytic degradation of dyes and antibiotics, Mater. Res. Express 9 (1) (2022) 015001.

[38] A.R. Khataee, F. Vafaei, M. Jannatkhah, Biosorption of three textile dyes from contaminated water by filamentous green algal Spirogyra sp.: kinetic, isotherm and thermodynamic studies, Int. Biodeterior. Biodegrad. 83 (2013) 33–40.

[39] R. Al-Tohamy, S.S. Ali, F. Li, K.M. Okasha, Y.A.G. Mahmoud, T. Elsamahy, H. Jiao, Y. Fu, J. Sun, A critical review on the treatment of dye-containing wastewater: ecotoxicological and health concerns of textile dyes and possible remediation approaches for environmental safety, Ecotoxicol. Environ. Saf. 231 (2022) 113160.

[40] P.A. Carneiro, G.A. Umbuzeiro, D.P. Oliveira, M.V.B. Zanoni, Assessment of water contamination caused by a mutagenic textile effluent/dyehouse effluent bearing disperse dyes, J. Hazard Mater. 174 (1–3) (2010) 694–699.

[41] M. Anvari, N. Shadjou, Dendritic fibrous nanosilica functionalized by dithiocarbamate as a highly efficient adsorbent for the removal of malachite green from waste water based on electrostatic interaction, Int. J. Environ. Sci. Technol. 18 (5) (2021) 1089–1096.

[42] K. Maheshwari, M. Agrawal, A.B. Gupta, Dye Pollution in Water and Wastewater. Novel Materials for Dye-Containing Wastewater Treatment, 2021, pp. 1–25.

[43] D. Wesenberg, I. Kyriakides, S.N. Agathos, White-rot fungi and their enzymes for the treatment of industrial dye effluents, Biotechnol. Adv. 22 (1–2) (2003) 161–187.

[44] H. Kumari, Suman Sonia, R. Ranga, S. Chahal, S. Devi, S. Sharma, S. Kumar, P. Kumar, S. Kumar, A. Kumar, A review on photocatalysis used for wastewater treatment: dye degradation, Water, Air, Soil Pollut. 234 (6) (2023) 349.

[45] D. Mantovania, H.B. Quesadaa, R. de Souza Antônioa, L.F. Cusiolia, L. Nishia, A. Diórioa, P.F. Soaresc, R. Bergamascoa, M.F. Vieiraa, Adsorption of methylene blue from effluent using golden mussel (Limnoperna fortunei) shell as a low-cost material, Desalination Water Treat. 188 (2020) 232–238.

[46] A.A.M. Sakib, S.M. Masum, J. Hoinkis, R. Islam, M. Molla, A. Islam, Synthesis of CuO/ZnO nanocomposites and their application in photodegradation of toxic textile dye, Journal of Composites Science 3 (3) (2019) 91.

[47] A. Tkaczyk, K. Mitrowska, A. Posyniak, Synthetic organic dyes as contaminants of the aquatic environment and their implications for ecosystems: a review, Science of the total environment 717 (2020) 137222.

[48] A.A. Peláez-Cid, S. Blasco-Sancho, F.M. Matysik, Determination of textile dyes by means of non-aqueous capillary electrophoresis with electrochemical detection, Talanta 75 (5) (2008) 1362–1368.

[49] R.R. Krishni, K.Y. Foo, B.H. Hameed, Adsorptive removal of methylene blue using the natural adsorbent-banana leaves, Desalination Water Treat. 52 (31–33) (2014) 6104–6112.

[50] S.I. Siddiqui, O. Manzoor, M. Mohsin, S.A. Chaudhry, Nigella sativa seed based nanocomposite-MnO2/BC: an antibacterial material for photocatalytic degradation, and adsorptive removal of Methylene blue from water, Environ. Res. 171 (2019) 328–340.

[51] F.A. Otieno, G.M. Ochieng, Water management tools as a means of averting a possible water scarcity in South Africa by the year 2025, WaterSA 30 (5) (2004) 120–124.

[52] T.L. Yusuf, B.O. Orimolade, D. Masekela, B. Mamba, N. Mabuba, The application of photoelectrocatalysis in the degradation of rhodamine B in aqueous solutions: a review, RSC Adv. 12 (40) (2022) 26176–26191.

[53] V.K. Gupta, I. Ali, V.K. Saini, T. Van Gerven, B. Van der Bruggen, C. Vandecasteele, Removal of dyes from wastewater using bottom ash, Ind. Eng. Chem. Res. 44 (10) (2005) 3655–3664.

[54] M.N. Alshabanat, M.M. AL-Anazy, An experimental study of photocatalytic degradation of Congo red using polymer nanocomposite films, J. Chem. 2018 (2018) 1–8.

[55] N. Nooraee Nia, M. Rahmani, M. Kaykhaii, M. Sasani, Evaluation of eucalyptus leaves as an adsorbent for decolorization of methyl violet (2B) dye in contaminated waters: thermodynamic and kinetics model, Modeling Earth Systems and Environment 3 (2) (2017) 825–829.

[56] D.A.G. Sumalinog, S.C. Capareda, M.D.G. de Luna, Evaluation of the effectiveness and mechanisms of acetaminophen and methylene blue dye adsorption on activated biochar derived from municipal solid wastes, J. Environ. Manag. 210 (2018) 255–262.

[57] H. Kolya, C.W. Kang, Toxicity of metal oxides, dyes, and dissolved organic matter in water: implications for the environment and human health, Toxics 12 (2) (2024) 111.

[58] C. Sahoo, A.K. Gupta, A. Pal, Photocatalytic degradation of Methyl Red dye in aqueous solutions under UV irradiation using Ag+ doped TiO_2, Desalination 181 (1–3) (2005) 91–100.

[59] M.A. Ahmad, N.A.B. Ahmed, K.A. Adegoke, O.S. Bello, Sorption studies of methyl red dye removal using lemon grass (Cymbopogon citratus), Chemical Data Collections 22 (2019) 100249.

[60] S. Begum, V.N. Narwade, D.I. Halge, S.M. Jejurikar, J.W. Dadge, S. Muduli, M.P. Mahabole, K.A. Bogle, Remarkable photocatalytic degradation of Remazol Brilliant Blue R dye using bio-photocatalyst 'nano-hydroxyapatite', Mater. Res. Express 7 (2) (2020) 025013.

[61] C. Purnawan, S. Wahyuningsih, O.N. Aniza, O.P. Sari, Photocatalytic degradation of remazol brilliant blue R and remazol yellow FG using TiO_2 doped Cd, Co, Mn, Bull. Chem. React. Eng. Catal. 16 (4) (2021) 804–815.

[62] Y. Liu, Y. Chen, Y. Shi, D. Wan, J. Chen, S. Xiao, Adsorption of toxic dye Eosin Y from aqueous solution by clay/carbon composite derived from spent bleaching earth, Water Environ. Res. 93 (1) (2021) 159–169.

[63] E. Alzahrani, Photodegradation of eosin Y using silver-doped magnetic nanoparticles, International journal of analytical chemistry 2015 (1) (2015) 797606.

[64] W. Zhang, X. Jiang, J. Ralston, J. Cao, X. Jin, W. Sun, Z. Gao, Efficient heterogeneous photodegradation of Eosin Y by oxidized pyrite using the photo-Fenton process, Miner. Eng. 191 (2023) 107972.

[65] M. Yu, Y. Han, J. Li, L. Wang, CO2-activated porous carbon derived from cattail biomass for removal of malachite green dye and application as supercapacitors, Chem. Eng. J. 317 (2017) 493–502.

[66] S.I. El-Hout, S.M. El-Sheikh, A. Gaber, A. Shawky, A.I. Ahmed, Highly efficient sunlight-driven photocatalytic degradation of malachite green dye over reduced graphene oxide-supported CuS nanoparticles, J. Alloys Compd. 849 (2020) 156573.

[67] G.K. Parshetti, S.G. Parshetti, A.A. Telke, D.C. Kalyani, R.A. Doong, S.P. Govindwar, Biodegradation of crystal violet by Agrobacterium radiobacter, Journal of environmental sciences 23 (8) (2011) 1384–1393.

[68] A. Ilyas, K. Rafiq, M.Z. Abid, A. Rauf, E. Hussain, Growth of villi-microstructured bismuth vanadate (Vm-BiVO 4) for photocatalytic degradation of crystal violet dye, RSC Adv. 13 (4) (2023) 2379–2391.

[69] R. Jasrotia, J. Prakash, G. Kumar, R. Verma, S. Kumari, S. Kumar, V.P. Singh, A.K. Nadda, S. Kalia, Robust and sustainable Mg1-xCexNiyFe2-yO4 magnetic nanophotocatalysts with improved photocatalytic performance towards photodegradation of crystal violet and rhodamine B pollutants, Chemosphere 294 (2022) 133706.

[70] Harita Kumari, Suman Sonia, Rohit Ranga, Surjeet Chahal, Seema Devi, Sourabh Sharma, et al., A review on photocatalysis used for wastewater treatment: dye degradation, Water, Air, Soil Pollut. 234 (6) (2023) 349.

[71] M.M. Hassan, C.M. Carr, A critical review on recent advancements of the removal of reactive dyes from dyehouse effluent by ion-exchange adsorbents, Chemosphere 209 (2018) 201–219.

[72] I. Anastopoulos, M.J. Ahmed, V.E. Ojukwu, M. Danish, M. Stylianou, J.O. Ighalo, A comprehensive review on adsorption of Reactive Red 120 dye using various adsorbents, J. Mol. Liq. (2023) 123719.

[73] M.M. Felista, W.C. Wanyonyi, G. Ongera, Adsorption of anionic dye (Reactive Black 5) using macadamia seed husks: kinetics and equilibrium studies, Scientific African 7 (2020) e00283.

[74] H.A. Tayebi, M. Ghanei, K. Aghajani, M. Zohrevandi, Modeling of reactive orange 16 dye removal from aqueous media by mesoporous silica/crosslinked polymer hybrid using RBF, MLP and GMDH neural network models, J. Mol. Struct. 1178 (2019) 514–523.

[75] A.M.S. Solano, C.A. Martínez-Huitle, S. Garcia-Segura, A. El-Ghenymy, E. Brillas, Application of electrochemical advanced oxidation processes with a boron-doped diamond anode to degrade acidic solutions of Reactive Blue 15 (Turquoise Blue) dye, Electrochim. Acta 197 (2016) 210–220.

[76] A. Esmaeili, A. Kalantari, Bioremoval of an azo textile dye, Reactive Red 198, by Aspergillus flavus, World J. Microbiol. Biotechnol. 28 (2012) 1125–1131.

[77] S. El Harfi, A. El Harfi, Classifications, properties and applications of textile dyes: a review, Applied Journal of Environmental Engineering Science 3 (3) (2017), 00000J-Envir.

[78] Z. Guan, Y. Wang, W. Chen, Y. Li, W. Yue, Z. Cai, Biodecolorization and biodegradation of sulfur black by the strain Aspergillus sp. DS-28, Processes 12 (9) (2024) 1818.

[79] J.H. Sun, S.P. Sun, G.L. Wang, L.P. Qiao, Degradation of azo dye Amido black 10B in aqueous solution by Fenton oxidation process, Dyes Pigments 74 (3) (2007) 647–652.

[80] A.E. Ali, Z.Z. Chowdhury, R. Devnath, M.M. Ahmed, M.M. Rahman, K. Khalid, Y.A. Wahab, I.A. Badruddin, S. Kamangar, M. Hussien, K.H. Pallan, Removal of azo dyes from aqueous effluent using bio-based activated carbons: toxicity aspects and environmental impact, Separations 10 (9) (2023) 506.

[81] N. Chinthalapudi, V.V.D. Kommaraju, M.K. Kannan, C.B. Nalluri, S. Varanasi, Composites of cellulose nanofibers and silver nanoparticles for malachite green dye removal from water, Carbohydrate Polymer Technologies and Applications 2 (2021) 100098.

[82] R. Sarathi, L.R. Devi, N.L. Sheeba, E.S. Esakki, S.M. Sundar, Photocatalytic degradation of malachite green dye by metal oxide nanoparticles-mini review, J. Chem. Rev 5 (1) (2023) 15–30.

[83] P. Geetha, M.S. Latha, M. Koshy, Biosorption of malachite green dye from aqueous solution by calcium alginate nanoparticles: equilibrium study, J. Mol. Liq. 212 (2015) 723–730.

[84] N. Thakur, N. Thakur, K. Kumar, V. Arya, A. Kumar, Encapsulation of Tinospora cordifolia plant in Ni doped TiO2 nanoparticles for the degradation of malachite green dye, Nanofabrication 8 (2023).

[85] C. Arora, P. Kumar, S. Soni, J. Mittal, A. Mittal, B. Singh, Efficient removal of malachite green dye from aqueous solution using Curcuma caesia based activated carbon, Desalination Water Treat. 195 (2020) 341–352.

[86] S. Shojaei, S. Shojaei, S.S. Band, A.A.K. Farizhandi, M. Ghoroqi, A. Mosavi, Application of Taguchi method and response surface methodology into the removal of malachite green and auramine-O by NaX nanozeolites, Sci. Rep. 11 (1) (2021) 1–13.

[87] X. Zhang, H. Yu, H. Yang, Y. Wan, H. Hu, Z. Zhai, J. Qin, Graphene oxide caged in cellulose microbeads for removal of malachite green dye from aqueous solution, J. Colloid Interface Sci. 437 (2015) 277–282.

[88] A. Elhalil, H. Tounsadi, R. Elmoubarki, F.Z. Mahjoubi, M. Farnane, M. Sadiq, M. Abdennouri, S. Qourzal, N. Barka, Factorial experimental design for the optimization of catalytic degradation of malachite green dye in aqueous solution by Fenton process, Water Resour. Ind. 15 (2016) 41–48.

[89] M.H.A. Elella, E.S. Goda, H. Gamal, S.M. El-Bahy, M.A. Nour, K.R. Yoon, Green antimicrobial adsorbent *containing grafted xanthan gum/SiO2 nanocomposites for malachite green dye. International Journal of Biological Macromolecules* 191 (2021) 385–395.

[90] A.L.D. da Rosa, E. Carissimi, G.L. Dotto, H. Sander, L.A. Feris, Biosorption of rhodamine B dye from dyeing stones effluents using the green microalgae Chlorella pyrenoidosa, J. Clean. Prod. 198 (2018) 1302–1310.

[91] M. Soylak, Y.E. Unsal, E. Yilmaz, M. Tuzen, Determination of rhodamine B in soft drink, waste water and lipstick samples after solid phase extraction, Food Chem. Toxicol. 49 (8) (2011) 1796–1799.

[92] G. Muthuraman, T.T. Teng, Extraction and recovery of rhodamine B, methyl violet and methylene blue from industrial wastewater using D2EHPA as an extractant, J. Ind. Eng. Chem. 15 (6) (2009) 841–846.

[93] S. Sharma, A.L.I. Imran, Adsorption of Rhodamine B dye from aqueous solution onto acid activated mango (Magnifera indica) leaf powder: equilibrium, kinetic and thermodynamic studies, J. Toxicol. Environ. Health Sci. 3 (10) (2011) 286–297.

[94] S. Singh, N. Parveen, H. Gupta, Adsorptive decontamination of rhodamine-B from water using banana peel powder: a biosorbent, Environ. Technol. Innovat. 12 (2018) 189–195.

[95] O.S. Bello, K.A. Adegoke, O.O. Sarumi, O.S. Lameed, Functionalized locust bean pod (Parkia biglobosa) activated carbon for Rhodamine B dye removal, Heliyon 5 (8) (2019) e02323.

[96] O.S. Bayomie, H. Kandeel, T. Shoeib, H. Yang, N. Youssef, M.M. El-Sayed, Novel approach for effective removal of methylene blue dye from water using fava bean peel waste, Sci. Rep. 10 (1) (2020) 1–10.

[97] M. Wainwright, K.B. Crossley, Methylene blue-a therapeutic dye for all seasons? J. Chemother. 14 (5) (2002) 431–443.

[98] F. Mashkoor, A. Nasar, Magsorbents: potential candidates in wastewater treatment technology–A review on the removal of methylene blue dye, J. Magn. Magn Mater. 500 (2020) 166408.

[99] C. Arora, S. Soni, S. Sahu, J. Mittal, P. Kumar, P.K. Bajpai, Iron based metal organic framework for efficient removal of methylene blue dye from industrial waste, J. Mol. Liq. 284 (2019) 343–352.

[100] J. Ibrahim, V.C. Ajaegbu, H.O. Egharevba, Pharmacognostic and phytochemical analysis of Commelina benghalensis L, Ethnobotanical Leaflets 2010 (5) (2010) 7.

[101] T.K. Sen, Adsorptive removal of dye (methylene blue) organic pollutant from water by pine tree leaf biomass adsorbent, Processes 11 (7) (2023) 1877.

[102] N. Fattahi, T. Fattahi, M. Kashif, A. Ramazani, W.K. Jung, Lignin: a valuable and promising bio-based absorbent for dye removal applications, Int. J. Biol. Macromol. (2024) 133763.

[103] L. Mouni, L. Belkhiri, J.C. Bollinger, A. Bouzaza, A. Assadi, A. Tirri, F. Dahmoune, K. Madani, H. Remini, Removal of Methylene Blue from aqueous solutions by adsorption on Kaolin: kinetic and equilibrium studies, Appl. Clay Sci. 153 (2018) 38–45.

[104] I. Khan, K. Saeed, I. Zekker, B. Zhang, A.H. Hendi, A. Ahmad, S. Ahmad, N. Zada, H. Ahmad, L.A. Shah, T. Shah, Review on methylene blue: its properties, uses, toxicity and photodegradation, Water 14 (2) (2022) 242.

[105] United States. Environmental Protection Agency, Office of solid waste, emergency response and tetra tech EM inc, in: Brownfields Technology Primer: Selecting and Using Phytoremediation for Site Cleanup, US Environmental Protection Agency, Office of Solid Waste and Emergency Response, 2001.

[106] S. Dawood, T.K. Sen, C. Phan, Synthesis and Characterization of novel-activated carbon from waste biomass pine cone and its application in the removal of Congo red dye from aqueous solution by adsorption, Water, Air, Soil Pollut. 225 (1) (2014) 1–16.

[107] S. Chawla, H. Uppal, M. Yadav, N. Bahadur, N. Singh, Zinc peroxide nanomaterial as an adsorbent for removal of Congo red dye from waste water, Ecotoxicol. Environ. Saf. 135 (2017) 68–74.

[108] K. Naseem, Z.H. Farooqi, R. Begum, A. Irfan, Removal of Congo red dye from aqueous medium by its catalytic reduction using sodium borohydride in the presence of various inorganic nano-catalysts: a review, J. Clean. Prod. 187 (2018) 296–307.

[109] N.S. Shah, J.A. Khan, M. Sayed, Z.U.H. Khan, J. Iqbal, S. Arshad, M. Junaid, H.M. Khan, Synergistic effects of H2O2 and S2O82− in the gamma radiation induced degradation of Congo-red dye: kinetics and toxicities evaluation, Separation and Purification technology 233 (2020) 115966.

[110] M.M. Iqbal, M. Imran, T. Hussain, M.A. Naeem, A.A. Al-Kahtani, G.M. Shah, S. Ahmad, A. Farooq, M. Rizwan, A. Majeed, A.R. Khan, Effective sequestration of Congo red dye with ZnO/cotton stalks biochar nanocomposite: MODELING, reusability and stability, J. Saudi Chem. Soc. 25 (2) (2021) 101176.

[111] R. Ramath, A.M. Sukumaran, A. Ramachandran, S.B. Basheer, Methyl orange dye adsorption and degradation at low temperature using iron oxide-incorporated biochar derived from industrial by-products, Bioresour. Technol. Rep. (2023) 101470.

[112] A. El Amri, L. Kadiri, R. Hsissou, A. Lebkiri, Z. Wardighi, A. Lebkiri, Investigation of Typha Latifolia (TL) as potential biosorbent for removal of the methyl orange anionic dye in the aqueous solution. Kinetic and DFT approaches, J. Mol. Struct. 1272 (2023) 134098.

[113] Z. Wang, Z. Chen, C. Ye, Enhancing methyl orange adsorption capacity via functionalizing ZIF-8 with amphiphilic cetylpyridinium bromide, J. Taiwan Inst. Chem. Eng. 146 (2023) 104865.

[114] M. Tu, J. Yu, J. Wang, X. Shi, Z. Fu, S. Hu, M. Zhong, Z. Fei, Coral-like TiO2/organosilane hybrid particles with rapid adsorption of methyl orange, Separ. Purif. Technol. 309 (2023) 123000.

[115] S.M. Alardhi, S.S. Fiyadh, A.D. Salman, M. Adelikhah, Prediction of methyl orange dye (MO) adsorption using activated carbon with an artificial neural network optimization modeling, Heliyon (2023) e12888.

[116] R. Ullah, M. Tuzen, Photocatalytic removal of organic dyes by titanium doped alumina nanocomposites: using multivariate factorial and kinetics models, J. Mol. Struct. 1285 (2023) 135509.

[117] M. Ravanan, M. Ghaedi, A. Ansari, F. Taghizadeh, D. Elhamifar, Comparison of the efficiency of Cu and silver nanoparticle loaded on supports for the removal of Eosin Y from aqueous solution: kinetic and isotherm study, Spectrochim. Acta Mol. Biomol. Spectrosc. 123 (2014) 467–472.

[118] M.S. Mansour, Y. Farid, S.A. Nosier, O. Adli, M.H. Abdel-Aziz, Removal of Eosin Yellow dye from industrial wastewater using UV/H2O2 and photoelectro-Fenton techniques, J. Photochem. Photobiol. Chem. 436 (2023) 114411.

[119] S.Y. Janbandhu, U. Patra, G.K. Sukhadeve, R. Kumar, R.S. Gedam, Photocatalytic performance of glasses embedded with Ag-TiO2 quantum dots on photodegradation of indigo carmine and eosin Y dyes in sunlight, Inorg. Chem. Commun. 148 (2023) 110317.

[120] F.A. Alharthi, A. Ali Alghamdi, H.S. Alanazi, A.A. Alsyahi, N. Ahmad, Photocatalytic degradation of the light sensitive organic dyes: methylene blue and rose bengal by using urea derived g-C3N4/ZnO nanocomposites, Catalysts 10 (12) (2020) 1457.

[121] M. Kurosu, K. Mitachi, E.V. Pershing, B.D. Horowitz, E.A. Wachter, J.W. Lacey III, Y. Ji, D.J. Rodrigues, Antibacterial effect of rose bengal against colistin-resistant gram-negative bacteria, J. Antibiot. 76 (7) (2023) 416–424.

[122] T.J. Al-Musawi, P. Rajiv, N. Mengelizadeh, I.A. Mohammed, D. Balarak, Development of sonophotocatalytic process for degradation of acid orange 7 dye by using titanium dioxide nanoparticles/graphene oxide nanocomposite as a catalyst, J. Environ. Manag. 292 (2021) 112777.

[123] C.J. Cooksey, Quirks of dye nomenclature. 15. Geranine—a simple name, with a less than straight forward identity, Biotech. Histochem. 95 (8) (2020) 613–618.

[124] H. Fu, K.A. Gray, TiO2 (Core)/Crumpled graphene oxide (shell) nanocomposites show enhanced photodegradation of carbamazepine, Nanomaterials 11 (8) (2021) 2087.

[125] A. Hussain, M.A. Altamimi, S. Alshehri, Green nanoemulsion (water/ethanol/triton X100/capmul MCM C8) to remove ciprofloxacin from a bulk aqueous solution, J. Mol. Liq. 345 (2022) 117863.

[126] X. Meng, Z. Qian, H. Wang, X. Gao, S. Zhang, M. Yang, Sol–gel immobilization of SiO2/TiO$_2$ on hydrophobic clay and its removal of methyl orange from water, J. Sol. Gel Sci. Technol. 46 (2) (2008) 195–200.

[127] L. Ai, H. Huang, Z. Chen, X. Wei, J. Jiang, Activated carbon/CoFe2O4 composites: facile synthesis, magnetic performance and their potential application for the removal of malachite green from water, Chem. Eng. J. 156 (2) (2010) 243–249.

[128] S. Benkhaya, S. M'rabet, A. El Harfi, A review on classifications, recent synthesis and applications of textile dyes, Inorg. Chem. Commun. 115 (2020) 107891.

[129] J.O. Unuofin, A.I. Okoh, U.U. Nwodo, Aptitude of oxidative enzymes for treatment of wastewater pollutants: a laccase perspective, Molecules 24 (11) (2019) 2064.

[130] M.S.S. Abujazar, S.U. Karaağaç, S.S.A. Amr, M.Y. Alazaiza, M.J. Bashir, Recent advancement in the application of hybrid coagulants in coagulation-flocculation of wastewater: a review, J. Clean. Prod. (2022) 131133.

[131] N.D.C.L. Beluci, G.A.P. Mateus, C.S. Miyashiro, N.C. Homem, R.G. Gomes, M.R. Fagundes-Klen, R. Bergamasco, A.M.S. Vieira, Hybrid treatment of coagulation/flocculation process followed by ultrafiltration in TiO$_2$-modified membranes to improve the removal of reactive black 5 dye, Sci. Total Environ. 664 (2019) 222–229.

[132] H. Liu, J. Zhang, M. Lu, L. Liang, H. Zhang, J. Wei, Biosynthesis based membrane filtration coupled with iron nanoparticles reduction process in removal of dyes, Chem. Eng. J. 387 (2020) 124202.

[133] T.H. Kim, C. Park, S. Kim, Water recycling from desalination and purification process of reactive dye manufacturing industry by combined membrane filtration, J. Clean. Prod. 13 (8) (2005) 779–786.

[134] M.B. Ahmed, J.L. Zhou, H.H. Ngo, W. Guo, Adsorptive removal of antibiotics from water and wastewater: progress and challenges, Sci. Total Environ. 532 (2015) 112–126.

[135] J. Fan, H. Li, C. Shuang, W. Li, A. Li, Dissolved organic matter removal using magnetic anion exchange resin treatment on biological effluent of textile dyeing wastewater, J. Environ. Sci. 26 (8) (2014) 1567–1574.

[136] M. Greluk, Z. Hubicki, Evaluation of polystyrene anion exchange resin for removal of reactive dyes from aqueous solutions, Chem. Eng. Res. Des. 91 (7) (2013) 1343–1351.

[137] P.C. Nnaji, V.C. Anadebe, I.G. Ezemagu, O.D. Onukwuli, Potential of Luffa cylindrica seed as coagulation-flocculation (CF) agent for the treatment of dye wastewater: kinetic, mass transfer, optimization and CF adsorption studies, Arab. J. Chem. 15 (2) (2022) 103629.

[138] M. Kaykhaii, M. Sasani, S. Marghzari, Removal of dyes from the environment by adsorption process, Chem. Mater. Eng 6 (2) (2018) 31–35.

[139] S. Ihaddaden, D. Aberkane, A. Boukerroui, D. Robert, Removal of methylene blue (basic dye) by coagulation-flocculation with biomaterials (bentonite and Opuntia ficus indica), J. Water Proc. Eng. 49 (2022) 102952.

[140] S.S. Moghaddam, M.A. Moghaddam, M. Arami, Coagulation/flocculation process for dye removal using sludge from water treatment plant: optimization through response surface methodology, J. Hazard Mater. 175 (1–3) (2010) 651–657.

[141] A. Szyguła, E. Guibal, M.A. Palacín, M. Ruiz, A.M. Sastre, Removal of an anionic dye (Acid Blue 92) by coagulation–flocculation using chitosan, J. Environ. Manag. 90 (10) (2009) 2979–2986.

[142] S. Wu, W. Shi, K. Li, J. Cai, C. Xu, L. Gao, J. Lu, F. Ding, Chitosan-based hollow nanofiber membranes with polyvinylpyrrolidone and polyvinyl alcohol for efficient removal and filtration of organic dyes and heavy metals, Int. J. Biol. Macromol. 239 (2023) 124264.

[143] T.M. Subrahmanya, J. Widakdo, S. Mani, H.F.M. Austria, W.S. Hung, H.K. Makari, J.K. Nagar, C.C. Hu, J.Y. Lai, An eco-friendly and reusable syringe filter membrane for the efficient removal of dyes from water via low pressure filtration assisted self-assembling of graphene oxide and SBA-15/PDA, J. Clean. Prod. 349 (2022) 131425.

[144] M. Zhu, Z. Cao, H. Yang, Z. Xu, C. Cheng, Improved dye and heavy metal ions removal in saline solutions by electric field-assisted gravity driven filtration using nanofiber membranes with asymmetric micro/nano channels, Separ. Purif. Technol. 300 (2022) 121775.

[145] J. Joseph, R.C. Radhakrishnan, J.K. Johnson, S.P. Joy, J. Thomas, Ion-exchange mediated removal of cationic dye-stuffs from water using ammonium phosphomolybdate, Mater. Chem. Phys. 242 (2020) 122488.

[146] M.I. Khan, A. Shanableh, A.M. Alfantazi, M.H. Lashari, S. Manzoor, R. Anwer, N. Farooq, F.A. Harraz, M. Alsaiari, M. Faisal, Application of QPPO/PVA based commercial anion exchange membrane as an outstanding adsorbent for the removal of Eosin-B dye from wastewaters, Chemosphere 321 (2023) 138006.

[147] X. Zhang, L. Hou, H. Liu, L. Chang, S. Lv, B. Niu, J. Zheng, S. Liu, J. Fu, Hollow polyphosphazene microcapsule with rigid-flexible coupling cationic skeletons for highly efficient and selective adsorption of anionic dyes from water, Appl. Surf. Sci. 626 (2023) 157234.

[148] D.D. Hu, Y.D. Li, Y. Weng, H.Q. Peng, J.B. Zeng, Mussel inspired stable underwater superoleophobic cotton fabric combined with carbon nanotubes for efficient oil/water separation and dye adsorption, Appl. Surf. Sci. 631 (2023) 157566.

[149] J.Y. Do, H. Moradi, D.S. Kim, J.K. Yang, Y.Y. Chang, S.S. Choi, Mesoporous biobased carbonaceous adsorbent for dye removal from water: eutectic molten salts effect and adsorption mechanisms, Diam. Relat. Mater. 136 (2023) 110018.

[150] S. Rani, S. Chaudhary, Adsorption of methylene blue and crystal violet dye from waste water using Citrus limetta peel as an adsorbent, Mater. Today: Proc. 60 (2022) 336–344.

[151] M.T. Yagub, T.K. Sen, S. Afroze, H.M. Ang, Dye and its removal from aqueous solution by adsorption: a review, Adv. Colloid Interface Sci. 209 (2014) 172–184.

[152] P. Krasucka, B. Pan, Y.S. Ok, D. Mohan, B. Sarkar, P. Oleszczuk, Engineered biochar–A sustainable solution for the removal of antibiotics from water, Chem. Eng. J. 405 (2021) 126926.

[153] L. Xin, J. Hu, X. Wu, K. Huang, X. Huang, Fenton-like degradation of carmine dyes based on artificial intelligence modeling and optimization of reduced graphene oxide loaded iron-cobalt-nickel trimetallic nanocomposites, Mater. Today Commun. (2022) 103463.

[154] A.A. Elbatea, S.A. Nosier, A.A. Zatout, I. Hassan, G.H. Sedahmed, M.H. Abdel-Aziz, M.A. El-Naggar, Removal of reactive red 195 from dyeing wastewater using electro-Fenton process in a cell with oxygen sparged fixed bed electrodes, J. Water Proc. Eng. 41 (2021) 102042.

[155] Y. Mao, Y. Zhao, S. Cotterill, Examining current and future applications of electrocoagulation in wastewater treatment, Water 15 (8) (2023) 1455.

[156] V. Kumar, M.P. Shah, Advanced oxidation processes for complex wastewater treatment, in: Advanced Oxidation Processes for Effluent Treatment Plants, Elsevier, 2021, pp. 1–31.

[157] W.H. Glaze, J.W. Kang, D.H. Chapin, The Chemistry of Water Treatment Processes Involving Ozone, Hydrogen Peroxide and Ultraviolet Radiation, 1987.

[158] X.H. Yang, S.Y. Sun, H.T. Fu, W.F. Li, X.Z. An, Two-step fabrication of porous α-Fe2O3@ δTiO$_2$ core-shell nanostructures with enhanced photocatalytic activity, in: 3rd Annual International Conference on Advanced Material Engineering (AME 2017), 2017, April, pp. 365–371.

[159] A.R. Ribeiro, O.C. Nunes, M.F. Pereira, A.M. Silva, An overview on the advanced oxidation processes applied for the treatment of water pollutants defined in the recently launched Directive 2013/39/EU, Environ. Int. 75 (2015) 33–51.

[160] M. Sillanpää, A. Matilainen, NOM removal by advanced oxidation processes, in: Natural Organic Matter in Water: Characterization and Treatment Methods, Butterworth-Heinemann, 2015, pp. 159–211.

[161] J. Meijide, P.S. Dunlop, M. Pazos, M.A. Sanromán, Heterogeneous electro-fenton as "Green" technology for pharmaceutical removal: a review, Catalysts 11 (1) (2021) 85.

[162] X. Ding, L. Gutierrez, J.P. Croue, M. Li, L. Wang, Y. Wang, Hydroxyl and sulfate radical-based oxidation of RhB dye in UV/H2O2 and UV/persulfate systems: kinetics, mechanisms, and comparison, Chemosphere 253 (2020) 126655.

[163] F. Qian, M. He, J. Wu, H. Yu, L. Duan, Insight into removal of dissolved organic matter in post pharmaceutical wastewater by coagulation-UV/H2O2, J. Environ. Sci. 76 (2019) 329–338.

[164] R. Arshad, T.H. Bokhari, T. Javed, I.A. Bhatti, S. Rasheed, M. Iqbal, A. Nazir, S. Naz, M.I. Khan, M.K.K. Khosa, M. Zia-ur-Rehman, Degradation product distribution of Reactive Red-147 dye treated by UV/H2O2/TiO$_2$ advanced oxidation process, J. Mater. Res. Technol. 9 (3) (2020) 3168–3178.

[165] K. Jutarvutikul, C. Sakulthaew, C. Chokejaroenrat, A. Pattanateeradetch, S. Imman, N. Suriyachai, T. Satapanajaru, T. Kreetachat, Practical use of response surface methodology for optimization of veterinary antibiotic removal using UV/H2O2 process, Aquacult. Eng. 94 (2021) 102174.

[166] D. Das, A. Bordoloi, M.P. Achary, D. Caldwell, R.P. Suri, Degradation and inactivation of chromosomal and plasmid encoded resistance genes/ARBs and the impact of different matrices on UV and UV/H2O2 based advanced oxidation process, Sci. Total Environ. (2022) 155205.

[167] N. Menek, C. Uğurlar, O. Uçarlı, Y. Karaman, S. Omanovic, S. Ghasemian, Degradation of calmagite by H$_2$O$_2$/UV/US, H$_2$O$_2$/US, H$_2$O$_2$, and US process, Alex. Eng. J. 61 (5) (2022) 4127–4135.

[168] G. Xue, M. Zheng, Y. Qian, Q. Li, P. Gao, Z. Liu, H. Chen, X. Li, Comparison of aniline removal by UV/CaO$_2$ and UV/H$_2$O$_2$: degradation kinetics and mechanism, Chemosphere 255 (2020) 126983.

[169] T.L. Shukla, S.J. Duranceau, Comparing hydrogen peroxide and sodium perborate ultraviolet advanced oxidation processes for 1, 4-dioxane removal from tertiary wastewater effluent, Water 15 (7) (2023) 1364.

[170] A.B. Ponnusami, S. Sinha, H. Ashokan, M.V. Paul, S.P. Hariharan, J. Arun, K.P. Gopinath, Q.H. Le, A. Pugazhendhi, Advanced oxidation process (AOP) combined biological process for wastewater treatment: a review on advancements, feasibility and practicability of combined techniques, Environ. Res. 237 (2023) 116944.

[171] M.M. Mohamed, I. Othman, R.M. Mohamed, Synthesis and characterization of MnOx/TiO$_2$ nanoparticles for photocatalytic oxidation of indigo carmine dye, J. Photochem. Photobiol. Chem. 191 (2–3) (2007) 153–161.

[172] D.A. Bopape, Z.N. Tetana, N. Mabuba, D.E. Motaung, N.C. Hintsho-Mbita, Biosynthesis of TiO$_2$ nanoparticles using Commelina benghanlensis for the photodegradation of methylene blue dye and antibiotics: effect of plant concentration, Results in Chemistry 5 (2023) 100825.

[173] Z.H. Xie, C.S. He, D.N. Pei, Y. Dong, S.R. Yang, Z. Xiong, P. Zhou, Z.C. Pan, G. Yao, B. Lai, Review of characteristics, generation pathways and detection methods of singlet oxygen generated in advanced oxidation processes (AOPs), Chem. Eng. J. 468 (2023) 143778.

[174] C. Jiang, W. Zhang, G. Zou, W. Yu, Y. Qian, Precursor-induced hydrothermal synthesis of flowerlike cupped-end microrod bundles of ZnO, J. Phys. Chem. B 109 (4) (2005) 1361–1363.

[175] G. Yang, Z. Yan, T. Xiao, Preparation and characterization of SnO2/ZnO/TiO2 composite semiconductor with enhanced photocatalytic activity, Appl. Surf. Sci. 258 (22) (2012) 8704–8712.

[176] V.N. Kalpana, V. Devi Rajeswari, A review on green synthesis, biomedical applications, and toxicity studies of ZnO NPs, Bioinorgan. Chem. Appl. 2018 (2018).

[177] A.A. Alshehri, M.A. Malik, Biogenic fabrication of ZnO nanoparticles using Trigonella foenum-graecum (Fenugreek) for proficient photocatalytic degradation of methylene blue under UV irradiation, J. Mater. Sci. Mater. Electron. 30 (17) (2019) 16156–16173.

[178] A.M. Tayeb, D.S. Hussein, Synthesis of TiO$_2$ nanoparticles and their photocatalytic activity for methylene blue, American Journal of Nanomaterials 3 (2) (2015) 57–63.

[179] V. Kumar, M. Gohain, S. Som, V. Kumar, B.C.B. Bezuindenhoudt, H.C. Swart, Microwave assisted synthesis of ZnO nanoparticles for lighting and dye removal application, Phys. B Condens. Matter 480 (2016) 36–41.

[180] Y. Li, W. Xie, X. Hu, G. Shen, X. Zhou, Y. Xiang, X. Zhao, P. Fang, Comparison of dye photodegradation and its coupling with light-to-electricity conversion over TiO$_2$ and ZnO, Langmuir 26 (1) (2010) 591–597.

[181] J.A. Quek, J.C. Sin, S.M. Lam, A.R. Mohamed, H. Zeng, Bioinspired green synthesis of ZnO structures with enhanced visible light photocatalytic activity, J. Mater. Sci. Mater. Electron. 31 (2) (2020) 1144–1158.

[182] A. Kumar, C.J. Raorane, A. Syed, A.H. Bahkali, A.M. Elgorban, V. Raj, S.C. Kim, Synthesis of TiO$_2$, TiO$_2$/PAni, TiO$_2$/PAni/GO nanocomposites and photodegradation of anionic dyes Rose Bengal and thymol blue in visible light, Environ. Res. 216 (2023) 114741.

[183] W.A. Mohamed, H.H. Abd El-Gawad, H.T. Handal, H.R. Galal, H.A. Mousa, B.A. ElSayed, A.A. Labib, M.S.A. Abdel-Mottaleb, Study of phytotoxicity, remarkable photocatalytic activity, recycling process and energy consumption cost of TiO$_2$ quantum dots photocatalyst for photodegradation of Coomassie brilliant blue R dye, Opt. Mater. 137 (2023) 113607.

[184] Y. Ge, H. Luo, J. Huang, Z. Zhang, Visible-light-active TiO$_2$ photocatalyst for efficient photodegradation of organic dyes, Opt. Mater. 115 (2021) 111058.

[185] Y.F. Li, W.P. Zhang, X. Li, Y. Yu, TiO$_2$ nanoparticles with high ability for selective adsorption and photodegradation of textile dyes under visible light by feasible preparation, J. Phys. Chem. Solid. 75 (1) (2014) 86–93.

[186] A.K. Aboul-Gheit, D.S. El-Desouki, R.A. El-Salamony, Different outlet for preparing nano-TiO$_2$ catalysts for the photodegradation of Black B dye in water, Egyptian Journal of Petroleum 23 (3) (2014) 339–348.

[187] S. Pavithra, T.C. Bessy, M.R. Bindhu, R. Venkatesan, R. Parimaladevi, M.M. Alam, J. Mayandi, M. Umadevi, Photocatalytic and photovoltaic applications of green synthesized titanium oxide (TiO$_2$) nanoparticles by Calotropis gigantea extract, J. Alloys Compd. 960 (2023) 170638.

[188] T. Tatarchuk, N. Danyliuk, A. Shyichuk, W. Macyk, M. Naushad, Photocatalytic degradation of dyes using rutile TiO$_2$ synthesized by reverse micelle and low temperature methods: real-time monitoring of the degradation kinetics, J. Mol. Liq. 342 (2021) 117407.

[189] R. Saini, P. Kumar, Green synthesis of TiO$_2$ nanoparticles using Tinospora cordifolia plant extract & its potential application for photocatalysis and antibacterial activity, Inorg. Chem. Commun. 156 (2023) 111221.

[190] D. Dodoo-Arhin, F.P. Buabeng, J.M. Mwabora, P.N. Amaniampong, H. Agbe, E. Nyankson, D.O. Obada, N.Y. Asiedu, The effect of titanium dioxide synthesis technique and its photocatalytic degradation of organic dye pollutants, Heliyon 4 (7) (2018) e00681.

[191] N.M. Ngoepe, M.M. Mathipa, N.C. Hintsho-Mbita, Biosynthesis of titanium dioxide nanoparticles for the photodegradation of dyes and removal of bacteria, Optik 224 (2020) 165728.

[192] X. Xue, W. Zang, P. Deng, Q. Wang, L. Xing, Y. Zhang, Z.L. Wang, Piezo-potential enhanced photocatalytic degradation of organic dye using ZnO nanowires, Nano Energy 13 (2015) 414–422.

[193] S. Chakrabarti, B.K. Dutta, Photocatalytic degradation of model textile dyes in wastewater using ZnO as semiconductor catalyst, J. Hazard Mater. 112 (3) (2004) 269–278.

[194] I. Kazeminezhad, A. Sadollahkhani, Photocatalytic degradation of Eriochrome black-T dye using ZnO nanoparticles, Mater. Lett. 120 (2014) 267–270.

[195] D. Dodoo-Arhin, T. Asiedu, B. Agyei-Tuffour, E. Nyankson, D. Obada, J.M. Mwabora, Photocatalytic degradation of Rhodamine dyes using zinc oxide nanoparticles, Mater. Today: Proc. 38 (2021) 809–815.

[196] K.A. Isai, V.S. Shrivastava, Photocatalytic degradation of methylene blue using ZnO and 2% Fe–ZnO semiconductor nanomaterials synthesized by sol–gel method: a comparative study, SN Appl. Sci. 1 (2019) 1–11.

[197] G. Yashni, A. AlGheethi, R.M.S.R. Mohamed, S.N.H. Arifin, V.A. Shanmugan, A.H.M. Kassim, Photocatalytic degradation of basic red 51 dye in artificial bathroom greywater using zinc oxide nanoparticles, Mater. Today: Proc. 31 (2020) 136–139.

[198] M. Golmohammadi, M. Honarmand, S. Ghanbari, A green approach to synthesis of ZnO nanoparticles using jujube fruit extract and their application in photocatalytic degradation of organic dyes, Spectrochim. Acta Mol. Biomol. Spectrosc. 229 (2020) 117961.

[199] S.S. Priyadharshini, J.P. Shubha, J. Shivalingappa, S.F. Adil, M. Kuniyil, M.R. Hatshan, B. Shaik, K. Kavalli, Photocatalytic degradation of methylene blue and metanil yellow dyes using green synthesized zinc oxide (ZnO) nanocrystals, Crystals 12 (1) (2021) 22.

[200] S. Chakraborty, J.J. Farida, R. Simon, S. Kasthuri, N.L. Mary, Averrhoe carrambola fruit extract assisted green synthesis of zno nanoparticles for the photodegradation of Congo red dye, Surface. Interfac. 19 (2020) 100488.

[201] F. Ameen, T. Dawoud, S. AlNadhari, Ecofriendly and low-cost synthesis of ZnO nanoparticles from Acremonium potronii for the photocatalytic degradation of azo dyes, Environ. Res. 202 (2021) 111700.

[202] H. AlMohamadi, S.A. Awad, A.K. Sharma, N. Fayzullaev, A. Távara-Aponte, L. Chiguala-Contreras, A. Amari, C. Rodriguez-Benites, M.A. Tahoon, H. Esmaeili, Photocatalytic activity of metal-and non-metal-anchored ZnO and TiO2 nanocatalysts for advanced photocatalysis: comparative study, Catalysts 14 (7) (2024) 420.

[203] S. Lin, L. Songyuan, F. Yaochong, Facile preparation of ZnO/TiO 2 nanocomposite photocatalysts and study of their photocatalytic performance, Journal of Ovonic Research 19 (6) (2023).

[204] J.Y. Park, J.H. Han, B.J. Choi, High-performance of ZnO/TiO2 heterostructured thin-film photocatalyst fabricated via atomic layer deposition, J. Vac. Sci. Technol. A 42 (3) (2024).

[205] G. Gelashvili, D. Gelenidze, D. Jishiashvili, Z. Shiolashvili, N. Makhatadze, A. Jishiashvili, V. Gobronidze, Photocatalytic activity of ZnO nanomaterials with different morphologies, Dig. J. Nanomater. Biostruct. 18 (3) (2023).

[206] N.N. Yunus, F. Hamzah, M.S. So'aib, J. Krishnan, Characterization and kinetic study of TiO2/ZnO Co-doped with nitrogen and sulphur at different calcination temperature, International Journal of Nanoelectronics and Materials (IJNeaM) 16 (December) (2023) 221–239.

[207] A. Azanaw, B. Birlie, B. Teshome, M. Jemberie, Textile effluent treatment methods and eco-friendly resolution of textile wastewater, Case Studies in Chemical and Environmental Engineering (2022) 100230.

[208] R. Taourati, M. Khaddor, A. El Kasmi, Stable ZnO nanocatalysts with high photocatalytic activity for textile dye treatment, Nano-Structures & Nano-Objects 18 (2019) 100303.

[209] T.G. Ambaye, K. Hagos, Photocatalytic and biological oxidation treatment of real textile wastewater, Nanotechnology for Environmental Engineering 5 (2020) 1–11.

[210] H. Pipil, S. Yadav, H. Chawla, S. Taneja, M. Verma, N. Singla, A.K. Haritash, Comparison of TiO$_2$ catalysis and Fenton's treatment for rapid degradation of Remazol Red Dye in textile industry effluent, Rendiconti Lincei. Sci. Fis. Nat. 33 (1) (2022) 105–114.

[211] D. Prabakar, V.T. Manimudi, T. Mathimani, G. Kumar, E.R. Rene, A. Pugazhendhi, Pretreatment technologies for industrial effluents: critical review on bioenergy production and environmental concerns, J. Environ. Manag. 218 (2018) 165–180.

[212] Y. Yang, J. Yang, J. Cao, Z. Wang, Pretreatment with concurrent UV photocatalysis and alkaline H2O2 enhanced the enzymatic hydrolysis of sisal waste, Bioresour. Technol. 267 (2018) 517–523.

[213] N.S. Ali, K.R. Kalash, A.N. Ahmed, T.M. Albayati, Performance of a solar photocatalysis reactor as pre-treatment for wastewater via UV, UV/TiO$_2$, and UV/H2O2 to control membrane fouling, Sci. Rep. 12 (1) (2022) 16782.

[214] C.Y. Chen, J.T. Kuo, H.A. Yang, Y.C. Chung, A coupled biological and photocatalysis pre-treatment system for the removal of crystal violet from wastewater, Chemosphere 92 (6) (2013) 695–701.

[215] J.X. Kang, L. Lu, W. Zhan, B. Li, D.S. Li, Y.Z. Ren, D.Q. Liu, Photocatalytic pre-treatment of oily wastewater from the restaurant by a vacuum ultraviolet/TiO$_2$ system, J. Hazard Mater. 186 (1) (2011) 849–854.

[216] I.A. Balcioglu, I. Arslan, Application of photocatalytic oxidation treatment to pre-treated and raw effluents from the Kraft bleaching process and textile industry, Environ. Pollut. 103 (2–3) (1998) 261–268.

[217] K. Sornalingam, A. McDonagh, J.L. Zhou, Photodegradation of estrogenic endocrine disrupting steroidal hormones in aqueous systems: progress and future challenges, Sci. Total Environ. 550 (2016) 209–224.

[218] M.N. Chong, B. Jin, Photocatalytic treatment of high concentration carbamazepine in synthetic hospital wastewater, J. Hazard Mater. 199 (2012) 135–142.